PB86-145802

Primary Photochemical Processes of Acrolein

National Center for Atmospheric Research
Boulder, CO

Prepared for

Environmental Protection Agency
Research Triangle Park, NC

Jan 86

U.S. Department of Commerce
National Technical Information Service
NTIS

PB86-145802

THE PRIMARY PHOTOCHEMICAL PROCESSES OF ACROLEIN

by

Edward P. Gardner, Paul D. Sperry
and Jack G. Calvert

National Center for Atmospheric Research
Box 3000, Boulder, Colorado 80307

Interagency Agreement DW 49930319

Project Officer
Joseph Bufalini

Atmospheric Physics and Chemistry Division
Atmospheric Sciences Research Laboratory
U.S. Environmental Protection Agency
Research Triangle Park, NC 27711

ATMOSPHERIC SCIENCES RESEARCH LABORATORY
OFFICE OF RESEARCH AND DEVELOPMENT
U.S. ENVIRONMENTAL PROTECTION AGENCY
RESEARCH TRIANGLE PARK, NORTH CAROLINA 27711

REPRODUCED BY
NATIONAL TECHNICAL
INFORMATION SERVICE
U.S. DEPARTMENT OF COMMERCE
SPRINGFIELD, VA. 22161

TECHNICAL REPORT DATA (Please read Instructions on the reverse before completing)		
1. REPORT NO. EPA/600/3-86/005	2.	3. RECIPIENT'S ACCESSION NO. PB86 145802/AS
4. TITLE AND SUBTITLE THE PRIMARY PHOTOCHEMICAL PROCESSES OF ACROLEIN		5. REPORT DATE January 1986 6. PERFORMING ORGANIZATION CODE
7. AUTHOR(S) Edward P. Gardner, Paul D. Sperry and Jack G. Calvert		8. PERFORMING ORGANIZATION REPORT NO.
9. PERFORMING ORGANIZATION NAME AND ADDRESS National Center for Atmospheric Research P. O. Box 3000 Boulder, Colorado 80307		10. PROGRAM ELEMENT NO. C9TA1B/01 - 2023 (FY-86) 11. CONTRACT/GRANT NO. IAG - DW49930319-01
12. SPONSORING AGENCY NAME AND ADDRESS Atmospheric Sciences Research Laboratory-RTP, NC Office of Research and Development U.S. Environmental Protection Agency Research Triangle Park, North Carolina 27711		13. TYPE OF REPORT AND PERIOD COVERED Final 14. SPONSORING AGENCY CODE EPA/600/09
15. SUPPLEMENTARY NOTES		

16. ABSTRACT

Pollutants are removed from the atmosphere in a number of ways: they can react with OH and O_3, they can be dry and wet deposited, photodissociate through solar radiation, or they can be biodegraded. This report presents the photodissociation processes of acrolein. Quantum yields of acrolein loss are given. The dominant reactions in the lower troposphere are the formation of C_2H_4 and CO. Also produced are CH_2 - CHCHO, H, CH_2CH, and HCO radicals but at lower quantum yields. Since the OH attack on acrolein is quite large (1.9×10^{-11} cm^3 $molec^{-1}$ s^{-1}) ambient levels of OH ($\sim 10^6$ molecules cm^{-3}) will remove acrolein very rapidly usually ~ 15 hours. Thus, the major loss mechanism of acrolein in the troposphere is through OH attack and the photodissociation process is of negligible importance.

17. KEY WORDS AND DOCUMENT ANALYSIS		
a. DESCRIPTORS	b. IDENTIFIERS/OPEN ENDED TERMS	c. COSATI Field/Group
18. DISTRIBUTION STATEMENT RELEASE TO PUBLIC	19. SECURITY CLASS (This Report) UNCLASSIFIED 20. SECURITY CLASS (This page) UNCLASSIFIED	21. NO. OF PAGES 22. PRICE

EPA Form 2220-1 (9-73)

NOTICE

The information in this document has been funded by the United States Environmental Protection Agency under Interagency Agreement DW 49930319 to the National Center for Atmospheric Research. It has been subject to the Agency's peer and administrative review, and it has been approved for publication as an EPA document.

Mention of trade names or commercial products does not constitute endorsement or recommendation for use.

ABSTRACT

The tropospheric concentration of a pollutant species is critically dependent upon the nature of the primary photochemical mechanism and the photooxidation product quantum yields. Previous investigations of acrolein photolysis, although qualitative, suggest an inefficient primary dissociation of acrolein (CH_2=CHCHO) excited at wavelengths within the region of the solar irradiated troposphere. The present study reports quantitative experiments designed to simulate closely tropospheric conditions. The dominant photolysis products are CO and C_2H_4 with quantum yields of 0.067 and 0.052 respectively, for 24.60 torr pressure (1.39% CH_2=CHCHO in synthetic air) of reaction mixture at 24.0 C°. The formation of C_2H_4 remained significant in spite of very high oxygen concentrations with increased synthetic air pressures, suggesting the molecular elimination of ethylene (and CO) as a major primary dissociative process. The approximate order of abundance of the quantified products is CO>C_2H_4>HCHO($\simeq H_2$)>HCOCHO>CO_2>CH_3OH($\simeq CH_4$). The mechanism most consistent with the thermochemistry and kinetics of the reaction species involves the formation of the excited singlet state of acrolein which rapidly undergoes molecular fragmentation to CO and C_2H_4 or, alternatively, can be collisionally deactivated to the excited triplet state, leading to the formation of $CH_3CH(T)$ and CO. This mechanism and computer simulations based on the experimental data indicate a very inefficient photochemical decomposition of acrolein under tropospheric conditions which can be summarized by the expression: $1/\Phi_A - 0.00400) = 0.086 + 613 \times 10^{-17}[M]$. This results in an estimated maximum apparent first order loss rate of $2.3 \times 10^{-6} s^{-1}$ for a solar zenith angle of 40 degrees.

CONTENTS

Abstract		iii
Figures		vii
Tables		ix
I.	Introduction	2
II.	Experimental Methods and Materials	5
	A. The Vacuum Line	5
	B. The Reaction Cell	8
	C. The Light Source	11
	D. Actinometry	15
	E. Photolysis	17
	1.) Light Absorption	17
	2.) Procedure	21
	F. Analysis	23
	1.) Sampling	23
	2.) Analytical System	24
	G. Source and Purity of Materials	31
III.	Results	34
	A. Product Quantum Yields	34
	1.) Calculation	34
	2.) Summary of Observations	41
IV.	Discussion	45
	A. Review of Previous Studies of Acrolein Photochemistry	45

Preceding page blank

B. Thermochemistry of the Possible Primary Processes in Acrolein Excited at 3130 Å in Air 51

C. Evidence from the Present Investigation Elucidating the Primary Processes of Acrolein Photolysis in Air 55

D. Computer Simulation of Product Quantum Yields in the 3130 Å Photolysis of Acrolein in Air 66

E. The Apparent First Order Photolytic Rate Coefficient for the Decay of Acrolein in the Lower Troposphere 78

V. Footnotes 83

VI. References 85

VII. Appendix 88

[Supplemental Stern-Volmer plots of product yields for 3130 Å photolysis of acrolein in air ∿ 25° C.]

FIGURES

Number		Page
1.	The vacuum line, illustrating the five major utility sections: (1) storage, (2) high/vacuum reference, (3) measurement, (4) calibration/mixture preparation, and (5) distillation.	6
2.	Frontal view of vacuum line with more detailed delineation of parts.	7
3.	The reaction cell for photolysis, showing direction/path of reaction mixture circulation	9
4.	The reaction cell showing construction and alignment of the photolysis train with the optical axis of the light source.	10
5.	Spectrum of the high-pressure mercury arc 1 amp (Osram, HBO 500 W/2).	13
6.	Transmission spectrum of narrow-band interference filter and absorption spectrum of acrolein.	14
7.	The UV absorption spectrum of acrolein in both units of atm^{-1} cm^{-1} (k, absorption coefficient at 0°C) and cm^{2} (σ, photoabsorption cross section); Varian/Cary 219 grating spectrophotometer using a 10 cm cell equipped with 2.5 cm diameter x 1.5 mm Sprasil windows	16
8.	Configuration of gas sampling values for delivery of the sample to the gas chromatograph (GC).	25
9.	Chromatographic separation of 313 nm photolysis of acrolein in synthetic air mixture.	27
10.	Calibrated gas inlet system to CEC model 21-104 mass spectrometer, equipped with a MKS Baratron (model 90M-XRP) capacitance manometer and 1-torr pressure head.	29
11.	Summary of the enthalpy relationships among the various electronic states of the acrolein molecule and the potential channels for reaction.	54

Number		Page
12.	Regression of the ratio [HCOCHO]/CH_2O] against [O_2] for 3130 Å photolysis of acrolein in air.	59
13.	Ratio of CO_2 to glyoxol (HCOCHO) vs pressure of added air for photolysis of acrolein at 3130 A.	64
	Comparison of simulated (crosses) and measured (squares) quantum yield of products and acrolein loss vs total pressure (torr) of reactant-air mixture.	
	Quantum Yield of:	
14.	Acrolein loss	71
15.	CO	72
16.	C_2H_4	73
17.	CO_2	74
18.	HCOCHO (glyoxal)	75
19.	CH_2O	76
20.	CH_3OH	77
21.	Contribution (quantum yield) of each of the primary processes to the total decomposition of acrolein at 3130 Å, as a function of total number of density (molecules cm^{-3}).	82

TABLES

Number		Page
1.	Useful wavelength ranges and product quantum yields for chemical actinometers employed.	18
2.	Summary of photolysis conditions λmax = 3130 Å.	35
3.	TCD molar responses of photolysis mixture components.	38
4.	Summary of quantum yields.	42
5.	Thermochemical data for selected species of importance in the photodissociation of acrolein.	52
6.	Proposed reaction mechanism for acrolein photolysis in air at 3130 Å.	67
7.	Estimated maximum J values for acrolein in the lower troposphere.	80

THE PRIMARY PHOTOCHEMICAL PROCESSES OF ACROLEIN

by

Edward P. Gardner, Paul D. Sperry
and Jack G. Calvert

National Center for Atmospheric Research*
P. O. Box 3000
Boulder, Colorado 80307

---

*The National Center for Atmospheric Research is sponsored by the National Science Foundation.

INTRODUCTION

The United States Environmental Protection Agency has identified a number of organic compounds as hazardous to human health. The relative abundance of these species in the ambient atmosphere is therefore of special concern. The rate processes which determine the tropospheric concentration of a particular compound are: (1) the rate and geographical distribution of its release into the troposphere; (2) the rate of its generation through tropospheric chemistry involving other precursor molecules in the atmosphere; (3) the rate of its removal via photochemical processes in the solar irradiated troposphere; (4) the rate of its removal by reactions with transient species, e.g., HO-radicals, O_3, etc., present in the troposphere; (5) the rates of its dilution and dispersion by atmospheric transport; (6) the rates of its dry and wet deposition on the Earth's surface; and (7) the rate of its degradation by microbial activity or other natural processes in the soil and aquatic environments. The intrinsic complexity and interdependency of these processes presuppose their full evaluation before a complete theoretical calculation of the tropospheric abundance of a chemical species can be achieved. However, among these, the nature of the primary photochemical mechanism and the photooxidation-product quantum yields, as elucidated in dilute, synthetic mixtures of air at pressures and temperatures commensurate with the troposphere, represent two processes upon which the prediction of the tropospheric concentration of a pollutant species

is critically dependent. This report presents the results of a quantitative investigation of the mechanism and quantum yields of the tropospheric photooxidation of acrolein, the simplest, unsaturated aldehyde and a potent lacrimator in polluted atmospheres.

Altshuller and McPherson (1963) and Kato and Hanai (1975) have reported atmospheric concentrations of Acrolein as high as 13 ppb or about 15% that of formaldehyde (Graedel, 1978). There are several previous investigations of acrolein, e.g.: Thompson and Linnett (1935), Blacet, Fielding, and Roof (1937), Harrison and Lossing (1959), Coomber and Pitts (1968), and Shinohara and Nishi (1982), which contribute evidence for the type and efficiency of its primary dissociative processes. The most pertinent quantitative investigation of the pure substance, that of Coomber and Pitts, at 313 nm, is consistent with an inefficient primary dissociation of acrolein excited at wavelengths within the region of the solar irradiated troposphere. Accordingly, it is anticipated that the primary dissociative pathways under tropospheric conditions are

$$CH_2{=}CHCHO + h\nu \rightarrow C_2H_4 + CO \qquad (I)$$

$$CH_2{=}CHCHO + h\nu \rightarrow C_2H_3 + HCO \qquad (II)$$

with quantum efficiencies which favor reaction (I) if dissociation occurs from the singlet excited state, or reaction (II) if dissociation is via the triplet state. The most recent study of Shinohara and Nishi (at 193 nm wavelength) strengthens the

hypothesis that reaction (II) should increase in importance with decreasing pressures of air, assuming dissociation from the vibrationally excited singlet. Osborne, Pitts, and Darley (1962) conducted a somewhat qualitative study of the stability of acrolein toward photooxidation, using relatively high pressures of reactant in oxygen. Although their study supports the hypothesis of inefficient tropospheric photo-destruction of acrolein, it does not provide the basis of a photochemical mechanism. A more detailed account of the previous investigations of acrolein will be provided in the discussion section of this report.[1] However, prior to the present study, no investigation of acrolein has been made with relatively low concentrations of reactant in air, at temperatures and pressures which reflect tropospheric conditions.

The set of experiments reported here were designed to closely simulate the conditions commonly encountered in the troposphere. Very small concentrations of acrolein were photolyzed with 313 nm ultraviolet light, reflecting the central wavelength region of the sunlight-irradiated troposphere, at approximately 25°C with synthetic air pressures salient to the troposphere. The results of this investigation represent the first available quantitative information on the primary quantum yields of acrolein photooxidation, and therefore provide the basis for the first realistic estimates of the photochemical loss rate of acrolein under tropospheric conditions.

EXPERIMENTAL METHODS AND MATERIALS

The Vacuum Line

A multifunctional gas-handling system, free of contaminating trace substances, was employed. This system is illustrated in Figures 1 and 2. As indicated, the vacuum line is comprised of five sections: (1) storage, (2) high vacuum/reference, (3) measurement, (4) calibration/mixture preparation, and (5) distillation. The storage section, located at the top of the vacuum line, consists of seven 5000 ml storage bulbs, each equipped with a cooling-stem to permit purification or distillation of the bulb contents. Pressure measurement is accomplished by a battery of MKS Baratron capacitance manometers, located beneath and to the left of the storage section, and by several thermocouple and Bayard-Alpert gauges distributed over the length of the vacuum line. Gases are introduced either by attaching glass bulbs of the desired gases directly to the system (via size 15 O-ring joints) or by opening the appropriate bellows-valve of the small manifold at the base of the calibration and mixture preparation section. The volumes of all parts of the measurement and calibration/mixture preparation sections were calibrated and are known, including those created by various combinations of open and closed valves. The distillation section consists of six chained dewar-traps to contain liquid nitrogen or other low-temperature baths and may be removed from the vacuum line for cleaning. The traps facilitate a thermally staged, serial distillation of contaminated and on-line manufactured gases. The

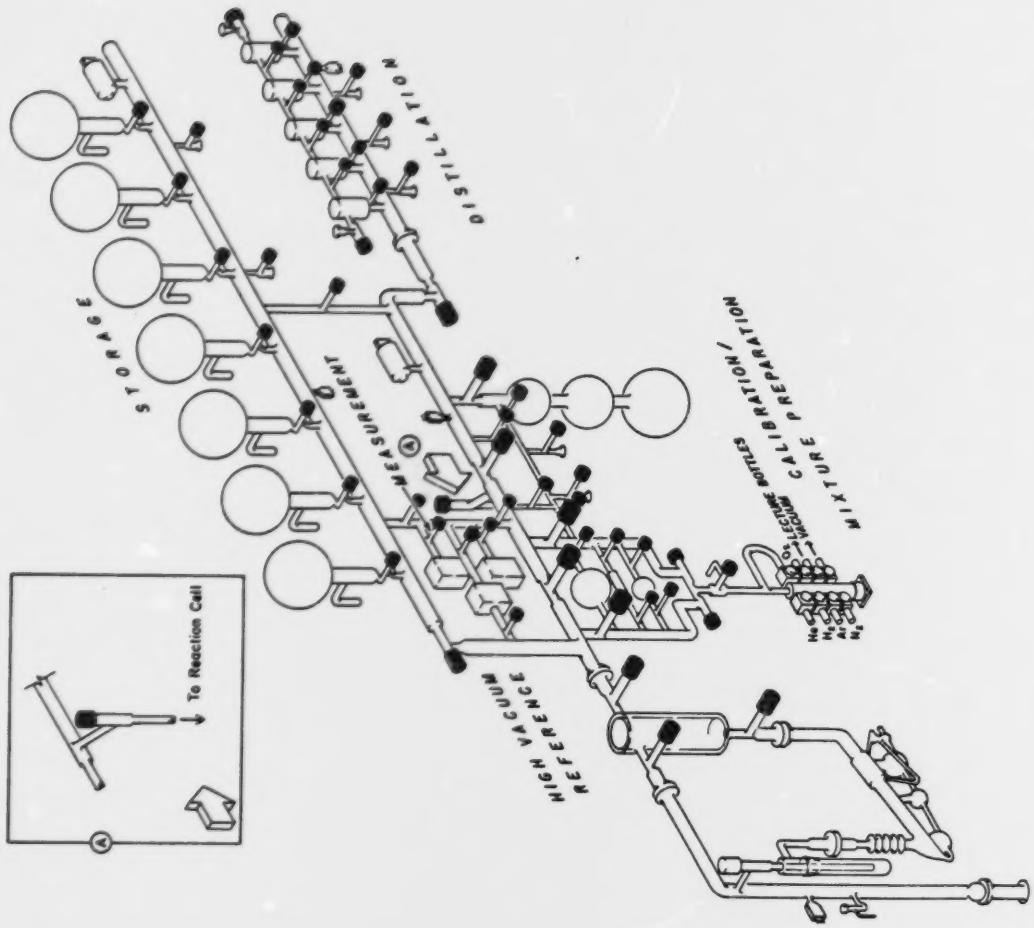

Figure 1. The vacuum line, illustrating the five major utility sections: (1) storage, (2) high/vacuum reference, (3) measurement, (4) calibration/mixture preparation, and (5) distillation.

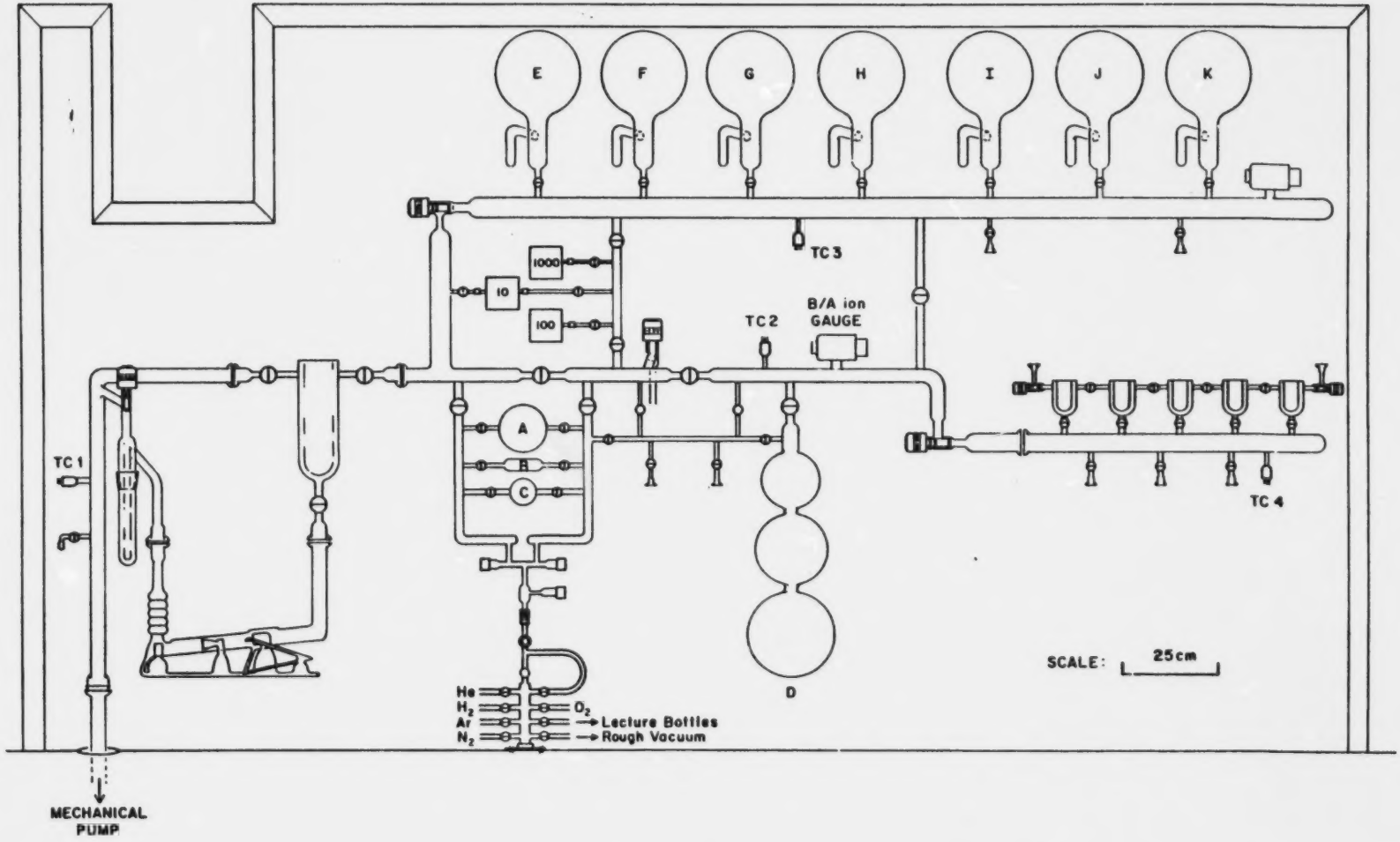

Figure 2. Frontal view of vacuum line with more detailed delineation of parts. E-K are 5000 ml storage vessels, A-C are calibrated volumes: 1000, 10.00 and 100.0 ml, respectively. D is a calibrated (10.0 liter) mixing vessel, equipped with a magnetically-driven winged stir bar.

purified gas is collected in glass bulbs (incorporating a cooling stem) by attaching the bulb, through a size 15 O-ring joint, to the distillation section. The system is pumped by a three-stage, glass, oil (Octoil) diffusion pump backed by a Duo-Seal mechanical pump (3000 litres min^{-1} at 1 mtorr). To increase pumping efficiency and protect the system from possible contamination by back-streaming oil vapor, a flow-through cold trap is included in the connecting line to the intake of the diffusion pump. All valves are greaseless, teflon-type with viton O-rings. Pressures of about $5X10^{-6}$ torr are normally achieved. The vacuum line connects directly to the reaction cell located on the other side of the vacuum rack (see insert, labeled A in Figure 1).

The Reaction Cell

The reaction cell, depicted in Figure 3, is designed to create an optically thin photochemical system with corresponding homogeneous reaction rates while maintaining a measurable conversion of the absorbing species. The internal optical path of the cell is 155.8 cm with Suprasil[2] windows fitted at the two ends. As indicated in Figure 4, each window is sealed with a low-vapor pressure epoxy cement[3] onto the ground end of an inner glass sleeve. The sleeve is ring-sealed into a size 75 O-ring joint which constitutes a cell end-piece. This configuration permits the windows to protrude inside the reaction cell, precluding a disparity between the temperature of the window and that of the cell interior. The end-pieces are easily demounted to allow the windows and the interior of the reaction cell to be cleaned. A narrow-band interference filter (313 nm) enclosed in a metal housing which

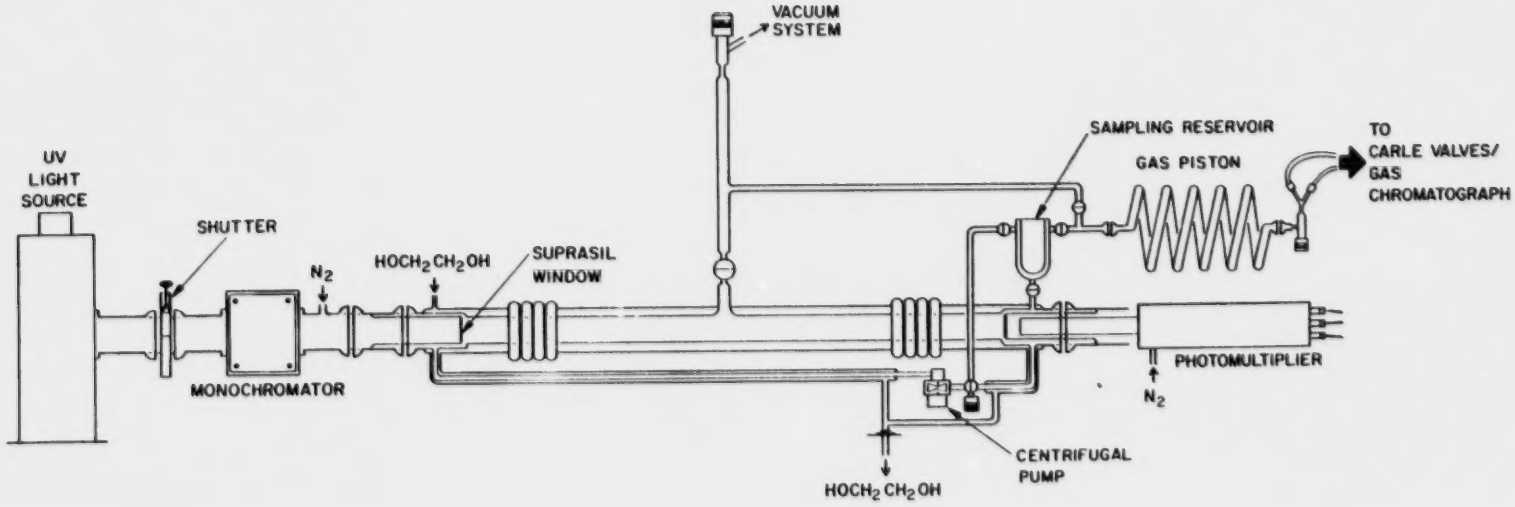

Figure 3. The reaction cell for photolysis, showing direction/path of reaction mixture circulation.

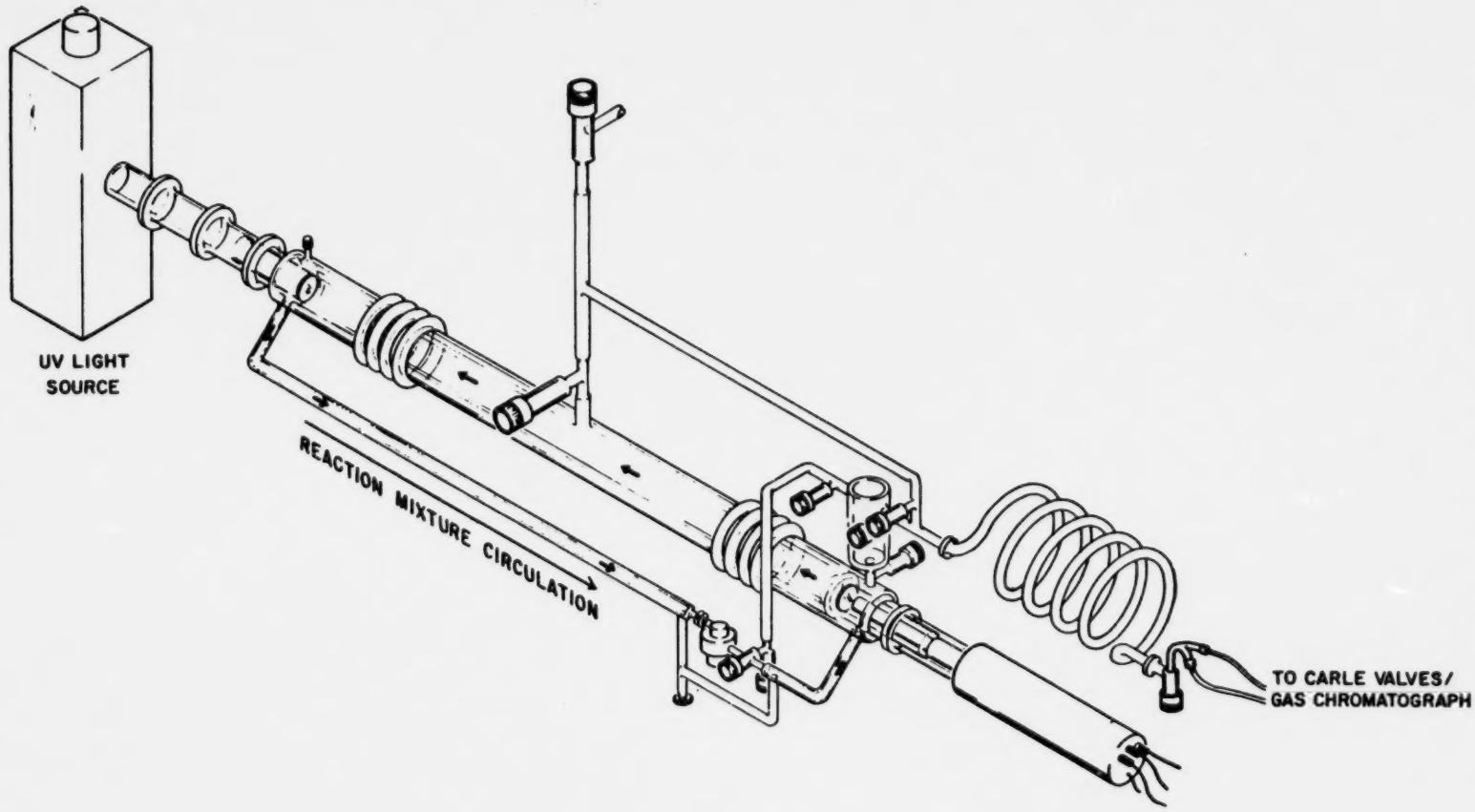

Figure 4. The reaction cell showing construction and alignment of the photolysis train with the optical axis of the light source.

duplicates the O-ring face of the cell end-pieces, is introduced into the optical train (as illustrated in Figure 4) to isolate the desired initiating wavelength. Alternatively, a Jarrell-Ash grating monochromator, purged with dry nitrogen gas, is inserted between the lamp housing and the photolysis cell to achieve a more precise isolation of the 313 nm wavelength; 2 mm entrance and exit slits are normally employed. The monochromator and lamp housing directly couple to the reaction cell in alignment with the optical train through gas-tight, metal, size 75 O-ring joints. A shutter, incorporating the design and dimensions of the interference filter assembly and manually activated to block the light path, is inserted between the O-ring faces in the optical train at the position closest to the lamp housing. The cell is enclosed in an outer jacket through which cooled or heated aqueous ethylene glycol is passed to maintain a constant temperature. A centrifugal pump, driven by an external rotating magnet, causes the reaction mixture to circulate as indicated by the arrows in Figure 3. Sampling is initiated by diverting the circulating reaction mixture into the dewar/sampling reservoir (not all of the valves are shown). The contents of the sampling reservoir can be sealed from the cell, fractionated and/or expanded into a "gas-piston" (the looped glass tube). Helium gas at about 900 torr pressure is admitted into the piston to compress the sample into a plug and drive it into the analytical system; e.g., a gas chromatograph. The volumes of all parts of the reaction cell and sampling system are known precisely.

The Light Source

The light source is a high-pressure mercury arc (Osram, HBO 500

W/2) enclosed in an Oriel, model C-60-51, lamp housing equipped with a quartz collimating lens. The lamp housing is modified to couple directly to the reaction cell in alignment with the optical train through a metal, size 75 O-ring joint.[4] Light exiting the reaction cell is intercepted by a model 8575 RCA photomultiplier tube (PMT) enclosed in a nitrogen-purged housing, equipped with narrow-band and neutral density filters. The photomultiplier output is transmitted to a Hewlett-Packard 5201L scaler-timer, digital pulse-height analyzer via a current to voltage, converter/amplifier (pulse output) and a separate pulse divider (range 4X - 4096X). The HP5201L pulse-height analyzer serves as a pulse totalizer of the photomultiplier output, providing a direct measure of the integrated light intensity transmitted over the photolysis time. The converter/amplifier circuit is housed within the PMT enclosure. An analog output is also available from the back of the PMT housing so that the PMT response can be directly observed with a laboratory chart recorder.[5] A voltage of -1100 volts is used to power the photomultiplier tube, resulting in a linear regression of pulse count against intensity for a given wavelength.

A spectrum of the high-pressure mercury arc lamp for wavelengths between 200 and 350 nm is provided in Figure 5. This may be compared with the transmission spectrum of the interference filter, shown in Figure 6, which was employed to isolate the region of the lamp output centered on the 313 nm (3.96 eV) mercury resonance line. For convenience, a scan of the relative absorption (arbitrary units) of light by acrolein in this region is included. A more complete absorption spectrum of acrolein in units of atm-1

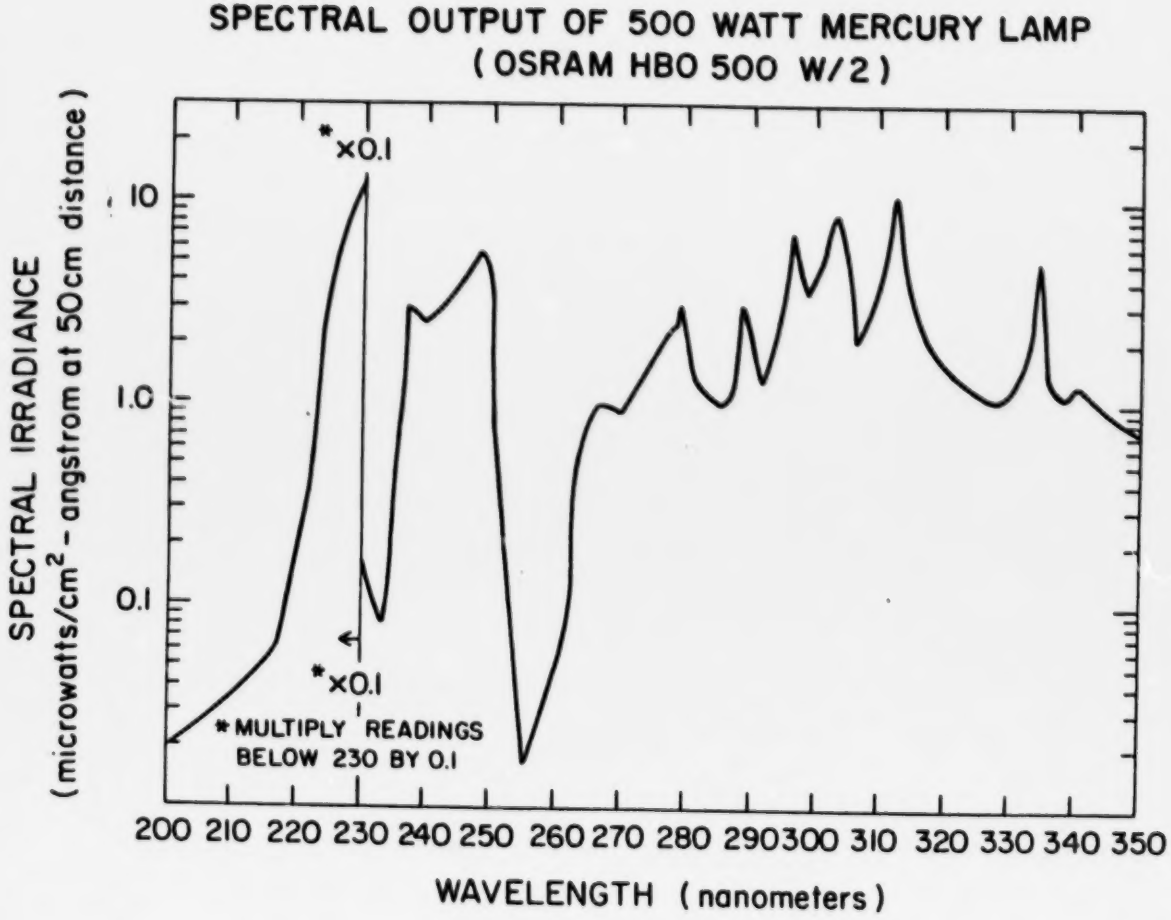

Figure 5. Spectrum of the high-pressure mercury arc lamp (Osram, HBO 500 W/2). Spectrum was from Oriel Corporation, Stamford, Connecticut.

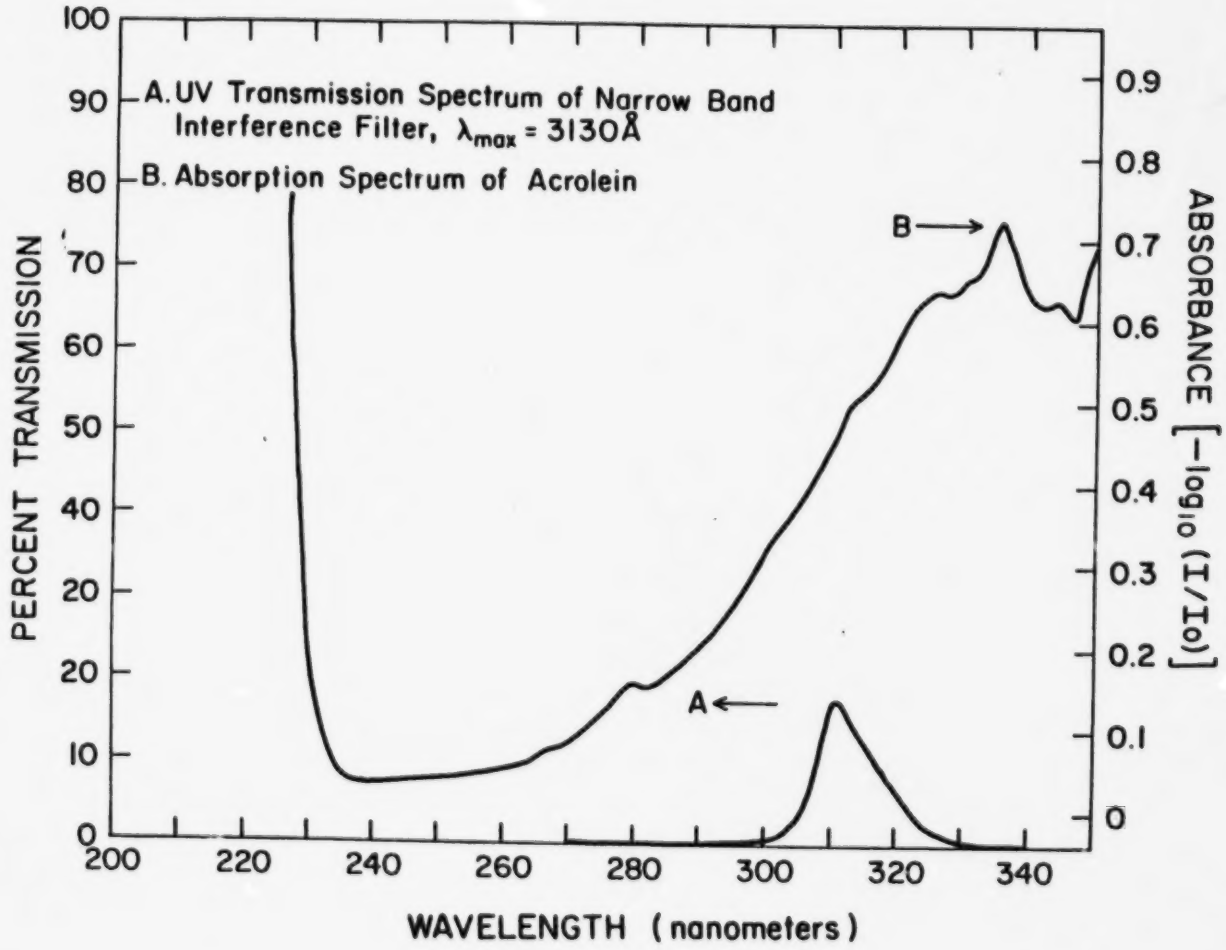

Figure 6. Transmission spectrum of narrow-band interference filter and absorption spectrum of acrolein.

cm-1 (k) and cm^2 (photoabsorption cross section, σ) is illustrated in Figure 7, utilizing the relations

$$k = \frac{(760 \text{ torr atm}^{-1}) \ln(I_t/I_o)}{-Pl}$$

and $$\sigma = k/\eta_o$$

where P is the pressure (torr) of the absorbing molecular species, l is the absorption path length, η_o is Loschmidt's number (2.69×10^{19} atm^{-1} cm^{-3}), and I_t and I_o are the transmitted and incident light intensities respectively. The spectral transmission of the filters and the absorption spectrum of acrolein were measured with a Varian/Cary 219 grating spectrophotometer. Discrete measurements of the effective photoabsorption cross sections of acrolein, corresponding to the transmission of the interference filter or of the (2 mm slits widths) monochromator, were made using the optical system of the reaction cell; e.g., see the solid (interference filter) and open (monochromator) circles in Figure 7 for 313 nm. Since the initiating light is not truly monochromatic, these in situ measurements insured the attainment of a reliable measure of the incident light intensity, and hence the total absorbed quanta in each experiment.

Actinometry

As previously indicated, the transmitted intensity of the initiating light is recorded during photolysis as an integrated pulse count representing the output of the photomultiplier. This is calibrated against a chemical actinometer by replacing the acrolein-

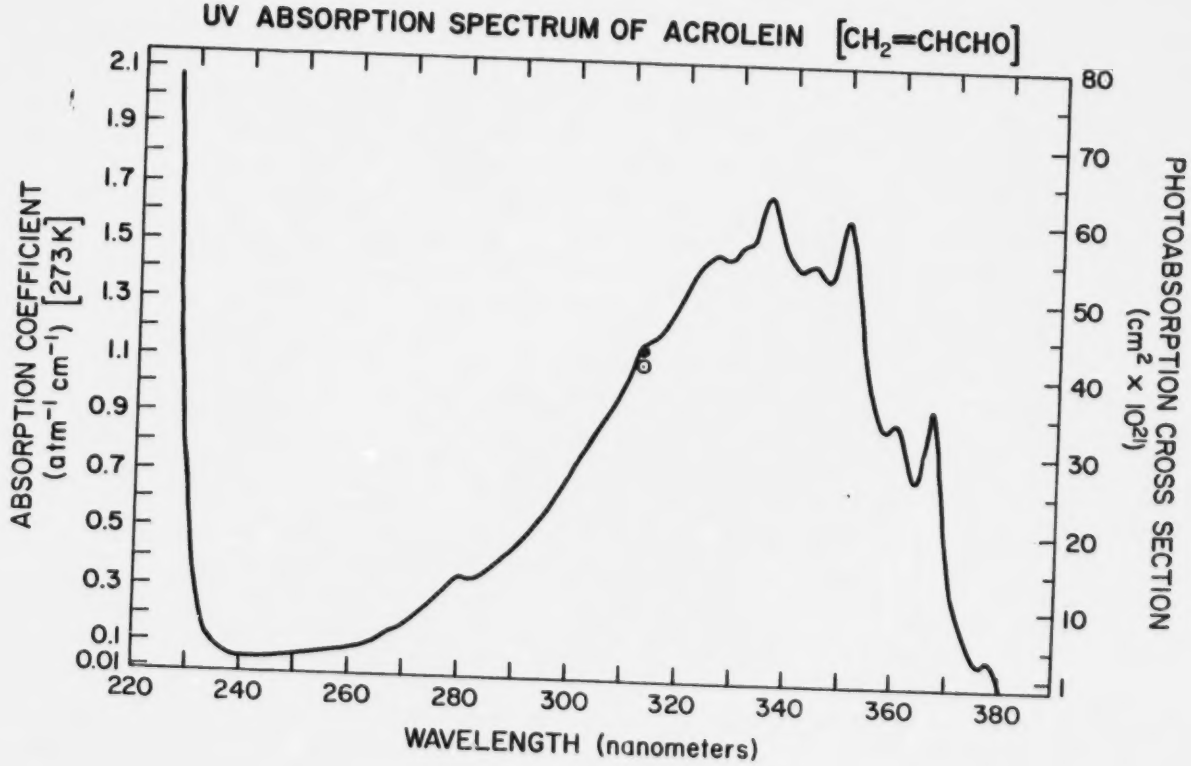

Figure 7. The UV absorption spectrum of acrolein in both units of $atm^{-1}cm^{-1}$ (k, absorption coefficient at $0^{o}C$) and cm^{2} (σ, photoabsorption cross section); Varian/Cary 219 grating spectrophotometer using a 10 cm cell equipped with 2.5 cm diameter x 1.5 mm Sprasil windows. The blackened and open circles represent the effective absorption coefficient/cross section at 3130 Å, measured using the interference filter and monochromator (2 mm slit widths), respectively. The circle diameters reflect the precision of the measurement.

air reaction mixture with an amount of actinometric reactant which transmits more than 90% of the incident light to the PMT. The total pulse count is translated into transmitted intensity by knowing the effective photoabsorption cross section of the actinometer, measured in the reaction cell, and the total absorbed quanta obtained from a quantitative analysis of the actinometric product and the corresponding known quantum yield.

Two chemical actinometers were employed: azomethane ($CH_3N{:}NCH_3$) and acetone (O_2 free); the actinometric products were N_2 and CO respectively. When azomethane was photolyzed, the total hydrocarbon yield was used as an additional check on the reliability of N_2 as the actinometric product. The useful wavelength range and product quantum yields are given in Table 1. By cross-referencing the two actinometers, an accuracy of 10% is estimated for acrolein quantum yield measurements with a reproducibility of better than $\pm$ 5%.

Photolysis

1. Light Absorption

It was stated that the design of the reaction cell facilitated an optically thin and therefore kinetically homogeneous photochemical system. The effect of this experimental condition in the photolysis of acrolein is briefly considered in the following paragraph.

Although the reaction mixture is composed of acrolein, oxygen, and nitrogen, the only absorbing species in the employed wavelength region is acrolein. Accordingly, for a system comprising a single absorbing species the integral form of the Beer-Lambert law is

TABLE 1. Useful wavelength ranges and product quantum yields for chemical actinometers employed

	Actinometer	range, nm	Φ	Comment	Reference
(1)	Acetone (O_2 free)	250-320	(CO) 1.0	T > 125°, P < 50 torr	Okabe, Photochemistry of Small Molecules, John Wiley and Sons, N.Y. (1978)
(2)	Azomethane	270-410 λ max = 340	(N_2) 1.0	T = 24-164C°	Steacie, Atomic and Free Radical Reactions, Reinhold, N.Y. (1954)

$$I_t/I_o = e^{-\eta\sigma l}$$

in which the ratio of the transmitted and incident light intensities per unit area is expressed as an exponential function of the negative product of the number of molecules per unit volume (η) of the absorbing species, its photoabsorption cross section (σ), and the total path length of the photolysis cell (l). Accordingly, the absorbed intensity per unit area (I_a) is calculated by solving for $I_o - I_t$, the difference between the incident and transmitted intensities:

$$I_o - I_t = I_o(1-e^{-\eta\sigma l}) = I_a$$

Assuming a collimated beam of light, the photolysis may be described as taking place within an effective volume delimited by the cross section of the light path times an effective path length (l_e), where the effective path length is determined by the magnitude of and . If I_a is the rate of absorption of quanta per unit area, then the average rate of light absorption per unit volume may be expressed by

$$R_{av} = I_a/l_e = I_o(1-e^{-\eta\sigma l})/l_e$$

The rate of light absorption and the rate of a primary photochemical process are related through the quantum yield (ϕ_p) of the process, defined as the number of reactant molecules dissociated by the primary process divided by the number of quanta absorbed by the reactant. Therefore, the average primary reaction rate (r_p) may be

written as

$$r_p = R_{av}\phi_p$$

If the absorbed fraction of the incident light is small, i.e., less than 10%, then it follows that the optical density ($\eta\sigma l$) is small and expansion of the exponential $e^{-\eta\sigma l}$ to a first term approximation results in

$$I_a/I_o = \eta\sigma l \text{ or } I_a = \eta\sigma l I_o$$

Accordingly, in the optically thin limit, the effective path length becomes the total path length of the cell and the rate of light absorption in the cell is said to be homogeneous. Therefore, the local and measured (average for the cell) reaction rates will be the same and can be expressed as

$$r_p = \eta\sigma l I_o \phi_p$$

This is the experimental condition established for the photolysis of acrolein in our laboratory. To consider an example, using the interference filter which has a maximum transmission at 313 nm, the average incident light intensity is 1.51×10^{15} quanta sec^{-1} cm^{-2}. The photolysis cell path length is 155.8 cm; η and σ for acrolein in the cell are 1.15×10^{16} molecules cm^{-3} and 4.09×10^{-20} cm^2 respectively. Therefore, for a primary dissociative process with a quantum yield of unity, the corresponding reaction rate locally and

throughout the photolysis cell is

$$r_p = 1.15\text{X}10^{16} \text{ X } 4.09\text{X}10^{-20} \text{ X } 1.51\text{X}10^{15}$$
$$r_p = 7.10\text{X}10^{11} \text{ molecules sec}^{-1} \text{ cm}^{-3}$$

2. Procedure

A calibrated reaction mixture of argon in acrolein (approximately 1:9.94) was prepared on the vacuum line prior to each experiment in which product hydrogen would be quantified by mass spectroscopy. Alternatively, for experiments in which hydrogen analysis was not conducted, either no internal standard was added or krypton was employed to create a calibrated mixture of Kr to acrolein of approximately 1:31.4. Confirmation of the accuracy of the calibrations was made by gas chromatography, establishing an absolute error of less than $\pm$0.6%.

The reaction cell is evacuated to less than $1\text{X}10^{-5}$ torr and filled with an actinometer at a pressure calculated to absorb >1% but <10% of the incident light. The actinometric reactant is typically exposed to the initiating light for a period of 240 minutes and product analysis conducted immediately afterward. The photomultiplier output, which was recorded (totalized) during photolysis, is indexed to the total transmitted intensity through the number of absorbed quanta and the fraction of absorbed light calculated from the product analysis, the established quantum yield for the actinometric product, and the measured effective photoabsorption cross section.

Once the photomultiplier is calibrated against one actinometer

(e.g., azomethane) for the light transmitted by the interference filter or monochromator, the experiment is repeated with a second actinometer (acetone) to access the accuracy of the intensity measured by the photomultiplier. The difference between the photometric and actinometric intensities suggests a random error of <10%.

In preparation for the photolysis of a mixture of acrolein and synthetic air, the reaction cell is heated (~100°C) and evacuated. The cooled (25°C) cell is then filled with the synthetic air mixture, without acrolein, and the cell contents circulated. This mixture is sampled and analyzed for the presence of contaminating species.[8] The cell is re-evacuated, the lamp ignited, and with the shutter open a five-minute pulse count of the photomultiplier output is recorded. This represents the incident intensity (I_o) on an arbitrary time base. A background count is recorded in the same manner except that the shutter mechanism is in the closed position. The cell (shutter closed) is then filled with an accurately measured pressure of acrolein (approximately 0.360 torr) or calibrated acrolein/argon mixture, followed by oxygen and, subsequently, nitrogen in the ratio of one to four, respectively, to constitute the added synthetic air. The total pressure of the air-acrolein mixture is an experimental variable, extending from 20 to 800 torr at 25°C. The cell contents are allowed to circulate for about 30 minutes to insure uniform mixing, followed by expansion into and circulation through the reservoir/sampling chamber. After an additional 15 minutes, the sampling chamber is sealed from the photolysis cell and the circulating reaction mixture rediverted to

the normal flow-path delineated in Figure 3. The pressure of the gas in the photolysis cell and in the sampling chamber are calculated using Boyle's law from the calibrated salient volumes and the filling pressure of the cell. The filling pressure for the staged addition of acrolein, oxygen, and nitrogen (total cell pressure) are measured with 0-1, 0-100, and 0-1000 torr heads respectively (MKS Baratron capacitance manometers). The aliquot of the unphotolyzed reactant mixture held in the reservoir/sampling chamber represents the control sample and is analyzed ahead of the photolyzed mixture after photolysis is complete.

Photolysis is initiated by setting the totalizer/timer of the HP5201L (pulse counter) for the anticipated photolysis time and simultaneously opening the shutter in the cell optical train. The digital (pulsed) output of the PMT is noted after the first five minutes of photolysis. The ratio of this number (I_t) to that recorded prior to filling the cell (I_o) provides an empirical measurement of the effective cross section of the reactant acrolein.

Analysis

1. Sampling

After photolysis, sampling is performed by diverting the flow of the circulating reaction mixture through the reservoir/sample chamber which incorporates a dewar-trap design. The sample chamber (76.52 ml volume) is sealed from the reaction cell and its contents cryogenically fractionated if required and/or expanded into the gas piston, a spiral tube (118 cm long X 2.5 cm diameter); see Figures 3 and 4. Helium gas in excess of one atmosphere pressure is admitted into the piston to compress the gas sample into a plug which is

received by a 3.0 ml, stainless steel, sample loop automatically evacuated between sampling cycles.

2. Analytical System

[Gas Chromatography]

The 3.0 ml sample loop, which in effect couples the analytical system to the sampling apparatus of the reaction cell, is switched into the chromatographic stream and subsequently re-evacuated in preparation for the next sampling cycle by a tandem of four electromechanically driven Carle, micro-volume, gas sampling valves controlled by a Hewlett-Packard 3390A computer/recorder. The microprocessor of the computer/recorder communicates the sampling schedule to the valves through a Carle, Series S_x, actuator-interface (which monitors the valve positions and permits manual override) and a Hewlett-Packard, "Sampler/event controller", digital to analog converter. The schedule and salient permutations of the valve configuration for delivery of the sample to the gas chromatograph (GC) are delineated in Figure 8. The use of a microprocessor controlled sample handling system to transfer and load an aliquot of the reaction mixture onto the GC column results in a highly reproducible chromatographic trace and hence, in reliable data.

A Varian, model 2700, gas chromatograph equipped with flame ionization (FID) and thermal conductivity (TCD) detectors was employed. The carrier gas (helium, 99.995% purity) is introduced into the gas chromatograph through the configured tandem of gas sampling valves after it is split into two streams (1 and 2 in Figure 8). Each stream passes through a pressure-controlled flow

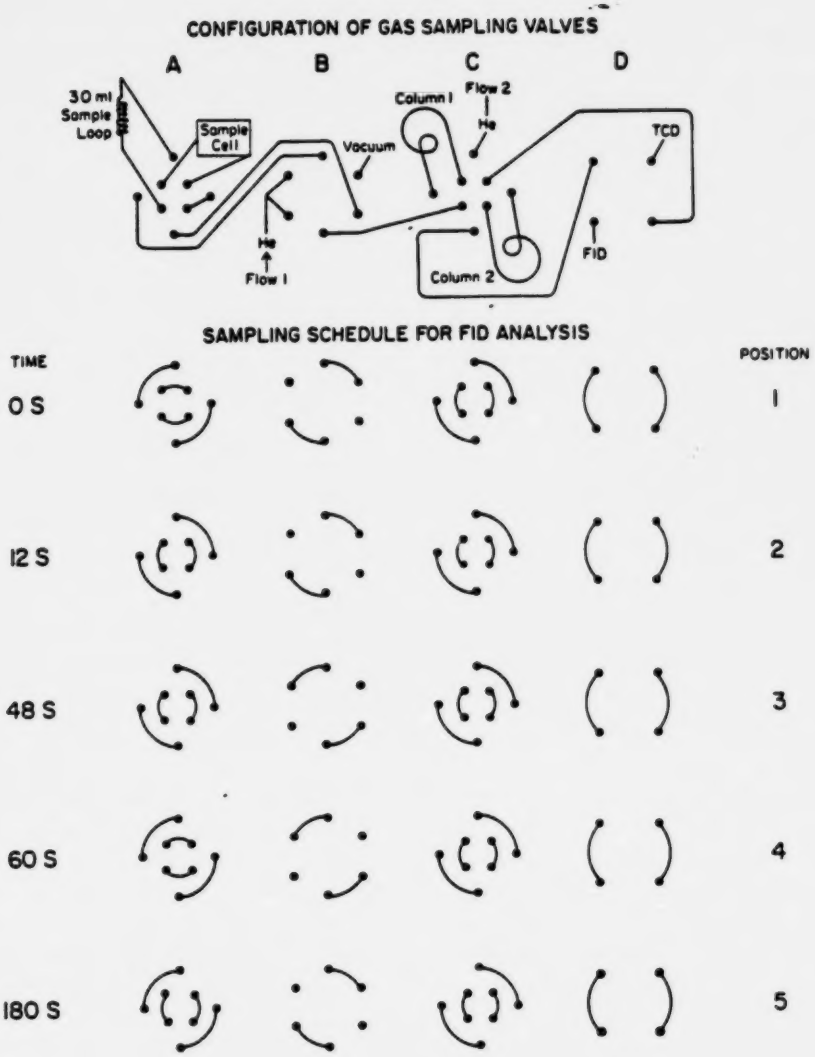

Figure 8. Configuration of gas sampling values for delivery of the sample to the gas chromatograph (GC). Lower portion of figure shows the sampling schedule and positions of values for FID analysis following chromatographic separation through column 1 (Porapak P/Q).

system which consists of a two-stage regulator, a capillary flow restrictor (calibrated to deliver a specific flow rate at a given regulator pressure) and a needle valve.

Two columns were used: 1. Porapak P/Q (mixture) 80/100 mesh, 70° C isothermal, 57 ml min^{-1} helium (carrier gas) 3.0 meter X 2.6 mm i.d.; and 2. Molecular Sieve 13X, 80/100 mesh, 50° and 75°C isothermal, 57 ml min^{-1} helium, 3.0 meter X 2.6 mm i.d.. The detector temperature was 200°C for all analyses. The two chromatographic streams (Figure 8) can be transferred to either column under microprocessor control and the two columns alternate with each other between normal and back-flushed positions with respect to the chromatographic stream as an automatic part of the sampling schedule. Similarly, the column effluent can be transferred to either detector, FID or TCD, according to the programmed schedule. These conditions provide both enhanced versatility of the chromatographic system and insurance against contamination of sequential chromatographic analyses by components with extended retention times.

Figure 9 is a chromatographic separation of a typical photolyzed mixture of acrolein in air. Reactant aliquots were loaded onto column one (Figure 8) Porapak P/Q, isothermal at 70°C, TCD and FID, sequentially. Under these conditions, Porapak P/Q effectively separates the photolysis products CH_4, CO_2, C_2H_4, HCHO, HOH, CH_3OH, CH_3CHO, HCOCHO, and residual reactant CH_2=CHCHO respectively. As indicated in Figure 9, if the effluent is switched to a flame ionization detector (see valve D in Figure 8) only those components which have a significant FID response would be observed;

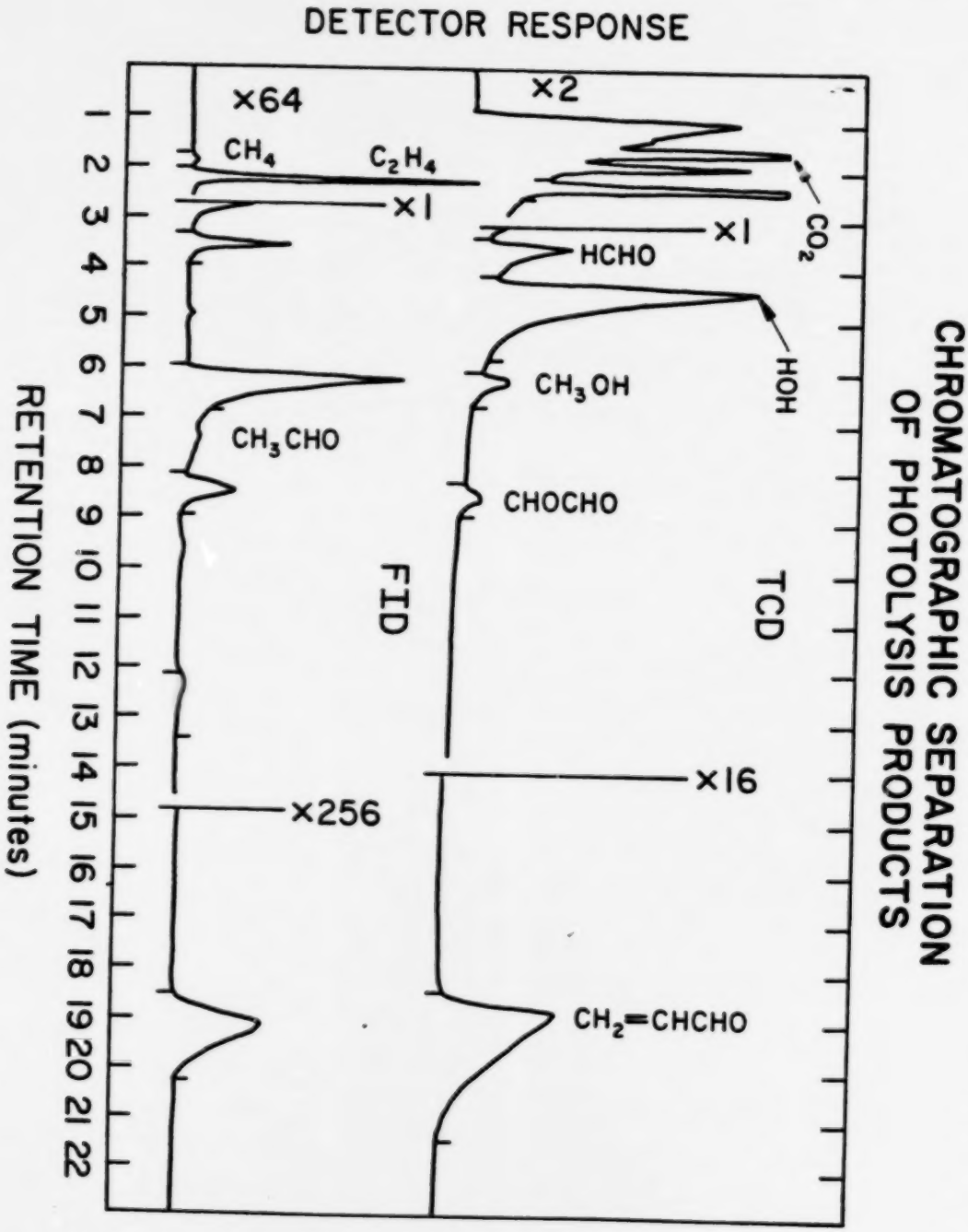

Figure 9. Chromatographic separation of 313 nm photolysis of acrolein in synthetic air mixture

i.e., CH_4, C_2H_4, HCHO, CH_3OH, CH_3CHO, HCOCHO, and CH_2=CHCHO. Hence, the ability to switch the column effluent to either detector without altering the chromatographic conditions greatly facilitates identification (and quantification) of the individual analytes. The second column in Figure 8, molecular sieve 13X, provides an exceptionally good separation of N_2, O_2, CO and the lighter C_1 - C_2 hydrocarbons.

The chromatographic peaks of product analytes were identified routinely by comparing their mean retention times with those obtained from GC analyses of pure gases and of commercially calibrated mixtures. Ancillary identification was made by observing their relative TCD and FID responses after a probable ID was established from the retention time. Additional inference of possible identities was obtained by cryogenic fractionation of the sampled reaction mixture prior to chromatographic analysis. Confirmation of the identity of an analyte was achieved by mass spectroscopy, after capturing the GC peak in the column effluent. Alternatively, if additional confirmation was required, pure gases - introduced into the sample chamber - were co-injected with the photolysis sample.

[Mass Spectroscopy]

Confirmation of the identity of GC analytes and quantification of product hydrogen was accomplished with a fully quantitative CEC model 21-104 mass spectrometer, interfaced with a calibrated gas inlet system (Figure 10) equipped with a MKS Baratron (Model 90M-XRP) capacitance manometer and 1-torr pressure head. Accordingly,

INLET SYSTEM TO MASS SPECTROMETER CEC 21-104

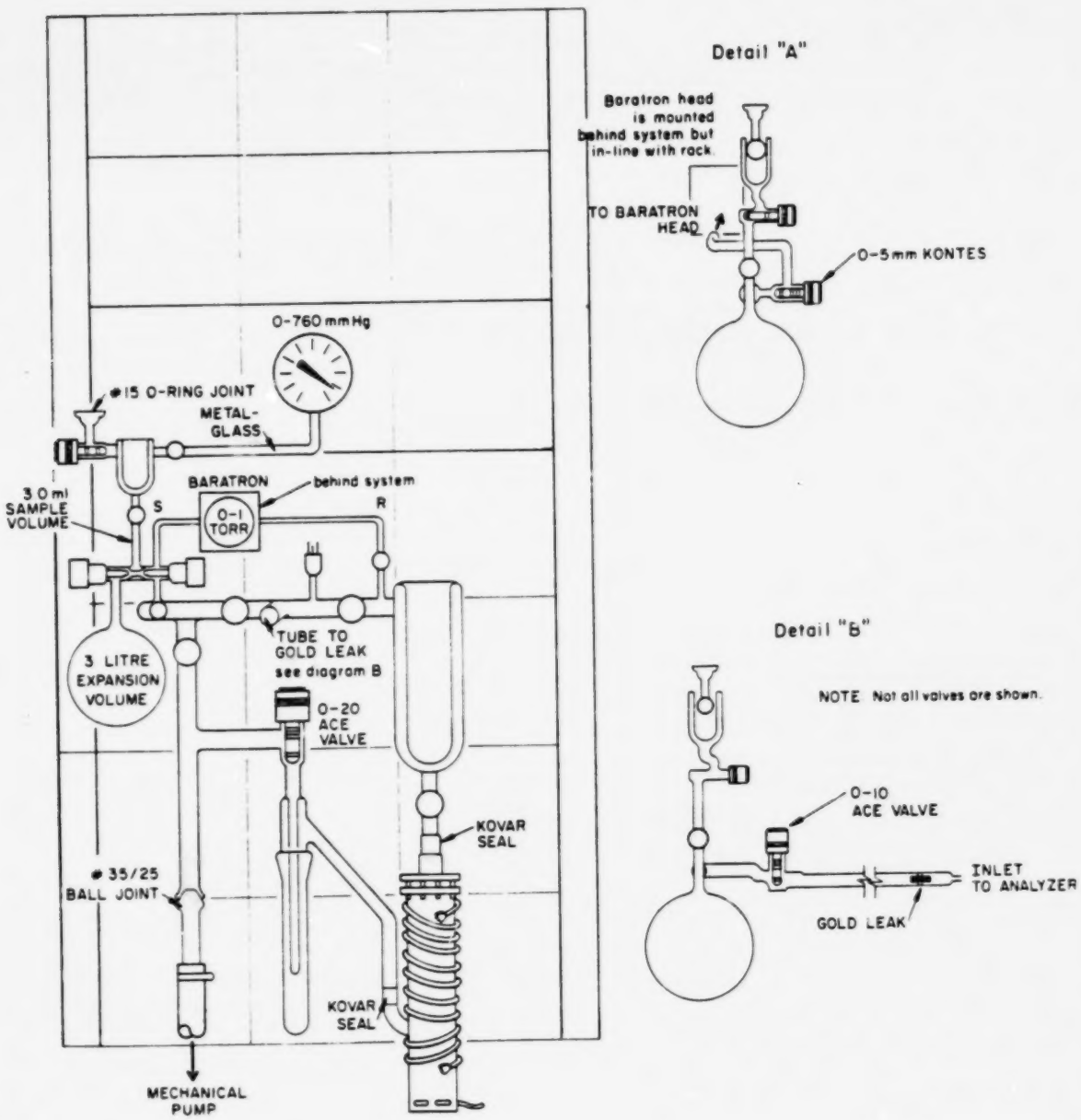

Figure 10. Calibrated gas inlet system to CEC model 21-104 mass spectrometer, equipped with a MKS Baratron (model 90M-XRP) capacitance manometer and 1-torr pressure head.

two analytical techniques were employed:

(1) For identification of of GC analytes, the unknown peak is captured cryogenically (~77 K) in a spiral glass capillary coil from the chromatographic effluent after passing the thermal conductivity detector. The glass coil, which is equipped with Kontes (0-5 mm) stopcocks at either end, is transferred from the GC to the mass spectrometer (MS) inlet system. The content of the coil is sequentially refrozen with liquid nitrogen, the volatile helium evacuated and the residual component (assuming the analyte is non-volatile at 77 K) revolatilized into the MS inlet system. Upon introducing the unknown substance through the molecular leak (gold leak) into the MS ionizing chamber, the inlet pressure is recorded and the mass spectrum of the substance scanned.

(2) For hydrogen analysis, an aliquot (~18 ml) of the photolyzed reaction mixture (adulterated with argon) is transferred to the mass spectrometer inlet system via a glass vial equipped with a break-seal. The vial is cooled with liquid nitrogen and product H_2 (accompanied by the other volatile [77 K] components of the reaction mixture) is expanded into the inlet system. Approximately 20 seconds after introduction of the volatile fraction into the MS ionizing chamber through the molecular leak, its pressure is measured with the capacitance manometer and a scan of M/e^- 2 + (14-80) is initiated.

All M/e^- scans are conveyed to an Apple //e computer utilizing an AI13, 12-bit analog to digital converter (Interactive Structures Inc., Bala Cynwyd, Pa. 19004) and a modified version of Dynamic Solutions Corporation chromatographic software [DSC] (Pasadena,

California 91101). The analog signal output from the mass spectrometer is digitized and treated according to the protocol established by the computer program; e.g., the M/e^- peaks are automatically identified and their amplitudes tabulated excluding background noise. The mass spectra are stored on 5.25" floppy disks for subsequent data reduction in software via Apple //e and Apple /// (256K) computers. A print-out of each spectrum is produced using the graphics module of the DSC software and an Epson dot-matrix printer. Alternatively, a record of the mass spectrum can be obtained directly from the MS using a fast response (<.25 second full scale deflection) four pen, Linseis, model LS-51, chart recorder.

Source and Purity of Materials

Reactant acrolein (CH_2=CHCHO) was obtained from Aldrich Chemical Company, Inc. (acrolein, 97% in water with 200 ppm hydroquinone). This commercial acrolein was purified by repeated distillations on the vacuum line and the middle third was collected in a blackened, 1-litre, glass storage bulb. Further purification was achieved by gas chromatography. Aliquots of the purified acrolein were analyzed by FID-gas chromatography (Porapak P/Q) and no impurity was detected. A minimum purity of 99.9% was established.

Oxygen and nitrogen were obtained from Linde (Union Carbide Corporation) and were of 99.99 (Ultra High Purity, Hydrocarbon Free grade) and 99.998% (Extra Dry grade) minimum purity respectively. Amounts of these gases, commensurate with a given photolysis run, were analyzed by TCD and FID gas chromatography, for HOH, CO_2, and

C-H-O species. As no contaminating substances were observed, the gases were used without further purification.

Carbon monoxide (CO) and carbon dioxide (CO_2) were obtained from Linde (Research Purity grade) and had stated minimum purities of 99.995 and 99.98% respectively.

Argon and Krypton were obtained in 1-litre glass bulbs (equipped with a break-seal) from Matheson at stated minimum purities of 99.995% and were used without further purification.

Azomethane was synthesized using the method of Renaud and Leitch.[9] The product was distilled on the vacuum line to achieve a reasonable purity.

Glyoxal (HCOCHO) was obtained as the trimeric Dihydrate ($C_6H_{10}O_8$) from Sigma Chemical Company and thermally decomposed to yield the monomer on the vacuum line. The monomer was used after distillation over P_2O_5 without further purification.

Reagent grade formaldehyde and glacial acetic acid were obtained from Eastman Kodak Company. Water ("distilled in glass", HPLC grade) and methanol (HPLC grade) were obtained from Burdick and Jackson Co.

Additional materials used as standards in the analysis (e.g., C_1-C_3 hydrocarbons and oxygen containing species) were obtained as Baker Analyzed Reagent grade and used without further purification.

Calibration mixtures of chromatographic standards: CO, CO_2, CH_4, O_2 (Scotty 1, analyzed gases 10-15% in nitrogen); C_1-C_6 alkanes and C_2-C_6 alkenes (Scotty 2 analyzed gases, each hydrocarbon mixture 100 ppm in helium) were obtained from Supelco, Inc.

The column chromatographic materials Porapak P/Q (80/100 mesh)

and molecular sieve 13X (80/100 mesh) were obtained from Alltech Associates, Inc.

RESULTS

As the principal objective of this investigation is to delineate the primary and secondary photochemical decomposition pathways of acrolein in Earth's troposphere and lower stratosphere, experiments were conducted which test the hypothesis of decreasing photo-decomposition with increasing atmospheric pressure. Accordingly, Table 2 summarizes the photolysis conditions: runs 1M-6M were conducted as a function of total pressure (20 to 800 torr) at a constant temperature of ~25°C with 313 nm initiating wavelength isolated by the Jarrell-Ash grating monochromator (2mm slits). Runs 7F-11F were performed under the same conditions of pressure and temperature with the 313 nm wavelength region of the mercury arc isolated by the narrow-band interference filter (Figure 6). All runs were conducted with approximately 0.355 torr of acrolein in synthetic air (~20% O_2 and 80% N_2).

Product Quantum Yields

1. Calculation

Of the eleven experiments conducted at 313 nm, three were performed with the intention of measuring the quantum yield of H_2. The experiment conducted at the lowest pressure of added air, Run #7F, is representative of this group and the data for it (see Table 2) are used to demonstrate the calculation of product quantum yields.

TABLE 2. SUMMARY OF PHOTOLYSIS CONDITIONS

λmax = 3130 Å

Run #	I_A Quanta	Filling Temp °C	Total Pressure torr	Mole Fraction of Acrolein	Mole Fraction of Nitrogen	Mole Fraction of Oxygen	Total Number Density molec cm^{-3}	Total Run Time min
1M	2.1911×10^{19}	22.75	658.29	5.3840×10^{-4}	0.79983	0.19963	2.1483×10^{19}	2341
2M	1.8694×10^{19}	24.60	79.221	4.4795×10^{-3}	0.80071	0.19436	2.5689×10^{18}	2100
3M	2.6468×10^{19}	23.42	524.67	6.7797×10^{-4}	0.80759	0.19173	1.7084×10^{19}	2610
4M	1.2858×10^{19}	22.80	25.540	1.3886×10^{-2}	0.79737	0.18874	8.3333×10^{17}	1200
5M	1.1724×10^{19}	22.35	790.85	4.4792×10^{-4}	0.79958	0.19997	2.5843×10^{19}	1621
6M	1.1363×10^{19}	24.25	359.46	9.8466×10^{-4}	0.79907	0.19995	1.1671×10^{19}	1620
7F	1.3261×10^{20}	24.08	25.607	1.3914×10^{-2}	0.78564	0.19905	8.3192×10^{17}	1620
8F	1.6889×10^{20}	25.80	359.96	9.8656×10^{-4}	0.80947	0.18954	1.1627×10^{19}	2770
9F	1.5464×10^{20}	24.34	110.43	3.20415×10^{-3}	0.79741	0.19906	3.6243×10^{18}	2351
10F	1.9265×10^{20}	23.28	231.79	1.53407×10^{-3}	0.79838	0.20008	7.5506×10^{18}	2340
11F	1.8918×10^{20}	25.42	47.523	7.44088×10^{-3}	0.81311	0.17870	1.5370×10^{18}	2359

Run #7F:

Photoabsorption path length (l) = 155.8 cm

Volume of reaction cell (V_R) = 4713.11 cm^3

Reaction cell filling temperature = 24.08°C

Total pressure of reaction mix = 25.607 torr

Total number density (η_T) = 8.3192 X 10^{17} molec cm^{-3}

Mole fraction of acrolein (x_r) = 1.3914 X 10^{-2}

Mole fraction of argon (x_a) = 1.3982 X 10^{-3}

Mole fraction of oxygen (x_o) = 0.19905

Mole fraction of nitrogen (x_n) = 0.78564

The number density of the absorbing species, acrolein, is obtained from the relation

$$\eta = \eta_T x_r$$

$$\eta = 1.1575 \text{ X } 10^{16} \text{ molec } cm^{-3} \quad .$$

The total quanta transmitted through the reaction cell (I_t) and the effective photoabsorption cross section of acrolein (σ) are 1.7328 X 10^{21} and 4.0892 X 10^{-20} cm^2, respectively. Therefore, the total absorbed quanta (I_a) is calculated by

$$I_a = I_t(e^{\eta\sigma l} - 1)$$

$$I_a = 1.3261 \text{ X } 10^{20} \text{ quanta} \quad .$$

Apple //e (128K RAM) and an Apple /// (256K RAM) computers were used to reduce the chromatographic data. Analysis of the calibrated mixtures of standards, conducted prior to analysis of the photolyzed reaction mixture, is reduced to molar response via the algorithm:[10]

$$n \text{ (nanomoles)} = \frac{P_s \times V_s \; V_p \; 10^9}{V_{(p+s)} \; RT \; 760 \text{ torr atm}^{-1}}$$

$$\text{molar response} = \frac{\text{Area units of component GC trace}}{\text{nanomoles (n) of component}}$$

The program utilizing this algorithm tests for the relative difference between the gas piston and reaction cell filling temperatures, branching to the appropriate step for correction to 0° C (273 K). Table 3 lists the reduced TCD molar responses of carbon monoxide, carbon dioxide, ethylene, formaldehyde, water, methanol, glyoxal, acrolein, and argon, respectively, for run #7F. The internal standard, argon, provides a convenient reference for normalization of the amounts of the individual components of the reaction mixture. For run #7F the normalized mean molar ratios of the components are:

CO	1.630
CO_2	0.2440
C_2H_4	1.260
HCHO	0.3417

TABLE 3

TCD MOLAR RESPONSES OF PHOTOLYSIS MIXTURE COMPONENTS

Component	Molar Response [AU/nanomole] [11]
CO	508.3
CO_2	629.5
C_2H_4	549.0
HCHO	269.5
HOH	262.0
CH_3OH	266.7
HCOCHO	209.0
CH_2=CHCHO	660.5
Ar	551.2

HOH	1.494
CH_3OH	0.1011
HCOCHO	0.1357
Acrolein (loss)	1.901
Argon	1.0
Hydrogen	0.2156

The number of argon atoms contained in the entire reaction mixture can be calculated:

$$N_{Ar} = V_R \eta_T x_a$$

$$= 4713.11 \times 8.3192 \times 10^{17} \times 1.3982 \times 10^{-3}$$

$$= 5.4822 \times 10^{18} \text{ atoms}$$

Accordingly, the number of molecules of each component or photolysis product in the reaction mixture may be obtained by multiplying its normalized (to Ar) molar ratio by the total number of argon atoms in the mixture:

Product	Number of molecules
CO	8.936×10^{18}
CO_2	1.338×10^{18}

C_2H_4	6.908×10^{18}
HCHO	1.873×10^{18}
HOH	8.190×10^{18}
CH_3OH	5.543×10^{17}
HCOCHO	7.439×10^{17}
Acrolein (loss)	1.042×10^{19}
Hydrogen	1.182×10^{18}

Alternatively, the total number of molecules of a product species may be calculated from the chromatographic data without reference to the internal standard by using the reaction cell filling pressure and pressure-volume relations of the sampling apparatus.

The product quantum yield (Φ) is defined as the number of molecules produced divided by the number of quanta absorbed by the reactant. Therefore, since the number of quanta absorbed in run #7F is 1.3261×10^{20}, from the previous tabulation the quantum yields of the photolysis products are:

Product	Φ
CO	0.0674
CO_2	0.0101
C_2H_4	0.0521
HCHO	0.0141
HOH	0.0618
CH3OH	0.00418

HCOCHO	0.00561
Acrolein (loss)	0.0786
Hydrogen	0.00891

2. Summary of Observations

A complete list of the product quantum yields for all runs (1M through 11F) is provided in Table 4. The regression of quantum yield and its reciprocal against total pressure (air) were plotted for each product. Quantum yield ratios were also plotted against total pressure to elucidate patterns of dependency which could distinguish secondary photolysis products from those originating in the primary mechanism. The resulting curves are provided in the Appendix. From these data the following principal observations are made:

1) The dominant products are CO and C_2H_4, respectively. The remaining quantified products are formaldehyde, hydrogen, glyoxal, carbon dioxide, methanol, and methane. The approximate order of abundance of these substances is:

$$CO > C_2H_4 > HCHO(\approx H_2) > HCOCHO > CO_2 > CH_3OH(\approx CH_4)$$

Trace amounts of acetaldehyde, acetylene, and acetic acid were also observed.

2) The formation of C_2H_4 is large in spite of very high oxygen concentrations, suggesting that the molecular elimination of C_2H_4 (and CO) must represent a major primary dissociative pathway. The other products, HCHO and HCOCHO in particular, are indicative of secondary O_2-association processes involving the CH_2CH and CH_3CH

TABLE 4. SUMMARY OF QUANTUM YIELDS

Run	Total Pressure	$\Phi_{CH_2=CHCHO}$	$\Phi_{C_2H_4}$	Φ_{CO_2}	Φ_{CO}	Φ_{CH_3OH}	Φ_{HCHO}	Φ_{HCOCHO}	Φ_{CH_4}	Φ_{H_2}
1M	658.29	0.00693	0.00181	0.00179	0.00533	0.000341	0.000533			
2M	79.221	0.0334	0.0121	0.00349	0.0244	0.00137	0.00583			
3M	524.67	0.00734	0.00193	0.00175	0.00589	0.000388	0.000610			
4M	25.540	0.0834	0.0523	0.0106	0.0714	0.00317	0.0149			
5M	790.85	0.00649	0.00177	0.0019		0.00036	0.00041			
6M	359.46	0.00909	0.00234	0.00171	0.00785	0.000477	0.000897			
7F	25.607	0.0786	0.0521	0.0101	0.0674	0.00418	0.0141	0.00561	0.0001909	0.00891
8F	359.96	0.00882	0.00244	0.00167	0.00823	0.000438	0.00100	0.00238		
9F	110.43	0.0257	0.00838	0.00273	0.0188	0.000625	0.00447	0.00200	0.0004522	0.00628
10F	231.79	0.0137	0.00346	0.00197	0.0102	0.000628	0.00126	0.00211	0.0010300	
11F	47.523	0.0681	0.0230	0.00566	0.0420	0.00376	0.00788	0.00306	0.0001300	

radicals.

3) As evidenced by the very small quantum yield of acrolein loss, the deactivation of excited acrolein is very efficient, presumably through the collisional transfer of vibrational energy to oxygen following intersystem crossing of the excited singlet to the triplet excited state.

4) The quantum yields of acrolein loss and product formation (with the exception of HCOCHO) decrease significantly with increasing pressure of air. However, even at pressures of approximately one atmosphere (760 torr) not all of the excited acrolein is quenched.

5) The presence of CH_4 among the products is indicative of the primary formation of the ethylidene (CH_3CH) radical, which oxidation could preface the reaction: $CH_3COOH^* \rightarrow CO_2 + CH_4$. However, this process is insufficient to explain the formation of CO_2, since the CO_2/CH_4 ratio is much greater than unity.

6) The CO/C_2H_4 quantum yield ratio increases with pressure from approximately 1.0 at pressures near 20 torr to ~3.0 at about 200 torr of added air, becoming approximately asymptotic at higher pressures.

7) Both the C_2H_4/CO_2 and CO/CO_2 ratios decrease with increasing pressure of added air. However, the C_2H_4/CO_2 ratio exhibits an exponential decrease relative to that of CO/CO_2 which is more nearly linear. A plot of CO/(Acrolein-loss) suggests a significant pressure dependent contribution of product CO via a secondary process.

8) The $(CO-C_2H_4)/C_2H_4$ quantum yield ratio increases with

pressure of added air, and becomes asymptotic at approximately 200 torr total pressure.

9) Unlike the other products, formaldehyde exhibits a linear Stern-Volmer plot; i. e., for the reciprocal of its quantum yield regressed against increasing air pressure. The obvious inference from this relation is that the decrease in HCHO production, relative to the other products, is due to its photolysis. Accordingly, the secondary photolysis of product formaldehyde must also be considered as a source of some of the observed products.

These observations are examined in the discussion section which follows.

DISCUSSION

Review of Previous Studies of Acrolein Photochemistry

It is well established that excitation at wavelengths within its first absorption band, beginning at about 3865 A, promotes the acrolein molecule to the first excited n,pi*, singlet state (S_1); see Brand and Williamson (1963) and Aves, Christoffersen, and Hollas (1971):

$$S_o + h\nu \rightarrow S_1$$

The weak absorption band of acrolein with its onset near 4120 A has been assigned to the transition of the ground state singlet to the first n,pi* triplet state:

$$S_o + h\nu \rightarrow T_1$$

Even under favorable conditions for emission, the radiative decay of excited acrolein is relatively unimportant. Becker, Inuzuka, and King (1970) reported a very small emission yield (0.004) from a fluid solution of acrolein at room temperature. Hansen (1973) has established an upper limit of 5×10^{-6} for the gas phase emission yield at room temperature and a pressure of 100 torr. The dominance of the nonradiative decay paths for excited acrolein may be rationalized following the suggestion of El-Sayed (1963, 1968) who demonstrated that in N-heterocycles, the S(n,pi*) -

$T(pi,pi^*)$ spin-orbit interaction is approximately 10^3 times that of the $S(n,pi^*)$ - $T(pi,pi^*)$ interaction. Based upon this evidence, Hansen and Lee (1973) have proposed that a similar phenomenon exists for the carbonyl compounds. More specifically, the spin-orbit interaction between the first excited singlet $S_1(n,pi^*)$ and second excited triplet $T_2(pi,pi^*)$ states may facilitate an efficient S_1 to T_2 intersystem crossing, followed by other radiationless processes, e.g., $T_2 \rightarrow T_1$.

In their review of aldehyde photochemistry, Lee and Lewis (1980) have concluded that the photodecomposition of excited acrolein is very inefficient. However, this conclusion is based upon quantum yield data derived from studies involving high pressures of acrolein for which deactivation of the excited states is especially efficient. The several previous investigations of acrolein photochemistry report a variety of products and propose many different reaction pathways which provide some insight into the complex mechanism of the oxygen-free photolysis of acrolein. As indicated in the introduction, the first studies of acrolein photodecomposition were reported by Thompson and Linnett (1935). In experiments performed at 3130 A with 145 torr of acrolein, they observed the gaseous products: CO (98.6%) and C_2H_4 (1.4%). Since polymerization of acrolein was extensive for their conditions, they proposed that the deficiency of carbon manifest in the product yields resulted from the absorption of C_2H_4 by the polymer deposited on the walls of the reaction vessel. Blacet, Fielding, and Roof (1937) observed similar results in experiments employing 200 torr of acrolein: i.e., 91% CO, 6% unsaturated compounds (presumably C_2H_4),

and 3% H_2. Accordingly, it was suggested that the dominant primary process involved free radical generation:

$$CH_2{=}CHCHO + h\nu \longrightarrow CH_2{=}CH + HCO \qquad (II)$$

The resulting HCO radicals could decompose to form H and CO, and the H-atoms and vinyl radicals would add to reactant acrolein to induce the observed polymer formation.

Harrison and Lossing (1959) studied the $Hg(^3P_1)$-sensitized decomposition of acrolein (2537 A, 112.7 kcal $mole^{-1}$) at very low (millitorr) pressures with product analysis by mass spectrometry. The distribution of the products observed was dependent on the length of the column of illumination and the extent of the decomposition. For the highest conversion (27.4%) the products were: CO, 54%; C_2H_4, 34%; and C_2H_2, 12%; for the lowest conversion (3.4%): CO, 55%; C_2H_4, 45%; and C_2H_2, 0%. Under these conditions, some butadiene was also observed as well as the radical combination products, $CH_2{=}CHCH_3$ and $CH_2{=}CHCOCH_3$, resulting from the generation of CH_3 radicals in the concurrent photosensitized decomposition of CH_3HgCH_3 with $CH_2{=}CHCHO$. The authors concluded that three primary processes must describe the $Hg(^3P_1)$-acrolein reaction:

$$Hg(^3P_1) + CH_2{=}CHCHO \longrightarrow CH_2{=}CH_2 + CO + Hg(^1S_o) \qquad (1)$$

$$\longrightarrow CH_2{=}CH + HCO + Hg(^1S_o) \qquad (2)$$

$$\longrightarrow CH_2{=}CHCO + H + Hg(^1S_o) \qquad (3)$$

Reaction (1) appears to be the major process, even though spin

inversion is required for this step to occur. Processes (2) and (3) are of minor importance.

Coomber and Pitts (1969) have carried out the most extensive investigation of the photodecomposition of acrolein at 3130 A, employing reactant pressures of 5 to 63 torr and temperatures between 35°and 200°C. They observed that the quantum yields of the major products, CO and C_2H_4, were dependent upon the pressure and temperature of the reaction mixture, composed of acrolein and either CO_2, piperylene, or NO. Self-quenching of the formation of gaseous products by acrolein was very evident: in experiments conducted at 126°C, the quantum yield of CO decreased from approximately 1.7×10^{-2} to 1.5×10^{-3} as the pressure was increased from 4.6 to 35 torr. The addition of CO_2 to the reaction mixture had little effect on the product yields; e.g., adding 307 torr of CO_2 to about 18 torr of acrolein only reduced the CO yield from 5.8×10^{-3} to 2.6×10^{-3}. In contrast, only small amounts of piperylene (1.9 torr) added to 4.6 torr of acrolein lowered the CO and C_2H_4 quantum yields to 77% and 61% or their piperylene-free values, respectively. However, the addition of 1.5 torr of NO to 18 torr of acrolein (125°C) resulted in a slight increase of the ethylene yield (2.8×10^{-3} to 3.3×10^{-3}). Therefore, the authors proposed that two primary processes occurred from the vibrationally excited, single state (S_1^*) for their conditions:

$$S_1^* \text{ --> } CO + C_2H_4 \qquad (4)$$

$$\text{--> } CH_2{=}CH + HCO \qquad (5)$$

$$\text{--> } T_1 \qquad (6)$$

In addition, the decomposition of the vibrationally relaxed, excited singlet state (S_1^o) in (7), the analogue to (5), followed by scavenging of the resulting vinyl radical by excess acrolein, was invoked to rationalize the absence of C_2H_4 at high reactant pressures. No analogue to (4) occurring from the S_1^o state was proposed.

$$S_1^o \text{ --> } CH_2{=}CH + HCO \qquad (7)$$

$$\text{--> } CH_2{=}CHCHO \qquad (8)$$

Since added piperylene, a triplet quencher, decreased the CO and C_2H_4 yields nearly the same extent, it was further proposed that the excited triplet could decompose via the spin forbidden process (9). Alternatively, the T_1 excited state could be quenched to the ground state in (10).

$$T_1 \text{ --> } C_2H_4 + CO \qquad (9)$$

$$\text{--> } CH_2{=}CHCHO \qquad (10)$$

In recent years, Umstead, Shortridge, and Lin (1978) and Shinohara and Nishi (1982) have investigated the mechanism of acrolein photolysis at short wavelengths (2000 and 1930 A) in which the initial excitation is to the second excited singlet (S_2, pi,pi*) state. Under these conditions, Umstead and coworkers observed that both methyl ketene ($CH_3CH{=}C{=}O$) and acrolein produce CO with similar, nonstatistical, vibrational distributions. As a result of a detailed consideration of these observations, they concluded that in

acrolein photolysis at energies sufficient to achieve the S_2 state a previously unsuspected primary process (11) is dominant:

$$CH_2{=}CHCHO + h\nu \rightarrow (CH_3CH{=}C{=}O) \rightarrow CH_3CH + CO \qquad (11)$$

Additional evidence for the occurrence of this primary process in acrolein photolysis has been provided very recently by Fujimoto, Umstead, and Lin (1985).

Shinohara and Nishi (1982) have observed vinyl and HCO radicals in the photodissociation of acrolein at 1930 A. The theoretical studies of Dykstra (1976), and Davidson and Nitzche (1979) reveal that the structure of the $S_2(pi,pi^*)$ state of the acrolein molecule, generated by excitation at 1930 A, involves a partial reversal of the bond order of the ground state. The C=C bond of the ground state acrolein molecule is lengthened by 0.13 A in the excited S_2 state, while the C-C bond adjacent to the carbonyl group is shortened, developing partial double-bond character and hence, precluding facile dissolution of C-C bond retaining the C=O group. Therefore, the formation of HCO and CH_2=CH radicals from the pi,pi^* excited state in acrolein photolysis is highly unlikely. Instead, the authors proposed that the dissociation occurs from the first excited $S_1(n,pi^*)$ surface to which the S_2 state degrades.

It is impossible to extrapolate the diverse and somewhat conflicting information in the literature to the conditions of the atmosphere, in which small reactant concentrations and high pressures of air predominate, to derive useful information on the photodecomposition modes and quantum efficiencies of acrolein

photolysis in the Earth's troposphere. In particular, a quantitative evaluation of the effect of oxygen on the primary photochemical processes has not be performed. The only previous work which even partially addresses this important problem is that of Osborne, Pitts, and Darley (1962) which demonstrates only in a very limited way that acrolein is particularly stable when irradiated in air.

Thermochemistry of the Possible Primary Processes in Acrolein excited at 3130 A in Air

Referring to the previous studies and the thermochemical constraints summarized in Table 5, one may evaluate the potential occurrence of several different photodecomposition modes for acrolein excited at wavelengths equal to or shorter than 3130 A:

$$CH_2{=}CHCHO + h\nu \longrightarrow S_1$$

$$S_1\ (+M) \longrightarrow T_1\ (+M)$$

$$S_1(\text{or } T_1) \longrightarrow CH_2{=}CH_2 + CO \qquad \text{(I)}$$

$$\longrightarrow CH_2{=}CH + HCO \qquad \text{(II)}$$

$$\longrightarrow CH_3CH(\text{Singlet}) + CO \qquad \text{(III)}$$

$$\longrightarrow CH_3CH(\text{Triplet}) + CO \qquad \text{(IV)}$$

$$\longrightarrow CH_2{=}CHCO + H \qquad \text{(V)}$$

$$T_1 + N_2 \longrightarrow S_o + N_2$$

$$T_1 + O_2(^3\Sigma_g^-) \longrightarrow S_o + O_2(^1\Sigma_g^+)$$

From Table 5, the minimum energy (kcal $mole^{-1}$) required for excited acrolein to decompose by the discrete processes, I through V, can be

TABLE 5

THERMOCHEMICAL DATA FOR SELECTED SPECIES OF IMPORTANCE IN THE PHOTODISSOCIATION OF ACROLEIN

Species	$\Delta H_f°$ (298 K), kcal mole^{-1}
CH_2=CHCHO	-18.32[a]
CH_2=CHCO	16.6[b]
CH_2=CH_2	12.50[c]
CH_3CH(Singlet)	91[d]
CH_3CH(Triplet, gd. state)	82[e]
CH_2=CH	69 $\pm$ 2[c]
HCO	9.0[c]
H	52.1[c]
CO	-26.42[c]

[a]Derived from the measured enthalpy of formation of liquid acrolein from Kharasch (1929) [Stull, Westrum, and Sinke, 1969] and the heat of vaporization of liquid acrolein listed by Reid, Prausnitz, and Sherwood (1977).

[b]Estimated assuming D(CH_2=CHCHO--H) = D(CHO--H) = 87 kcal/mole.

[c]Benson (1976).

[d]Calculated from the data of Umstead et al. (1978) and an assumed singlet-triplet energy gap of 9 kcal/mole, Borden and Davidson (1979).

[e]Umstead et al. (1978); estimate is assumed to refer to the CH_3CH species in the ground (triplet) state.

estimated to be: 4, 96, 82, 73, and 87 kcal $mole^{-1}$, respectively. For photochemical initiation at 3130 A and a temperature of 298 K, the newly excited singlet state of acrolein will have 91.4 kcal $mole^{-1}$ of electronic energy, in addition to respective average translational, rotational, and vibrational energies of 1.9, 1.9, and 1.6 kcal $mole^{-1}$. Accordingly, at 298 K, the mean total internal energy available to the acrolein molecule which absorbs a quantum of light of 3130 A wavelength is 95 kcal $mole^{-1}$.

In Figure 11 we have summarized the enthalpy relationships among the various electronic states of the acrolein molecule and the potential channels for product formation. In principle, each of the primary processes, I-V, could occur from the initially excited singlet species formed at 3130 A. However, as vibrational relaxation occurs in the excited singlet state, it is apparent that vinyl and formyl radical generation in (II) is precluded energetically. More specifically, this energy constraint requires that dissociation by process (II) can only occur shortly after excitation, before significant relaxation of the vibrational modes can be accomplished.

The product quantum yields reported in the present study represent an important contribution of new information concerning the nature of the processes which occur in the photodecomposition of acrolein in air. In the following section, these data are considered in the formulation of a reaction mechanism.

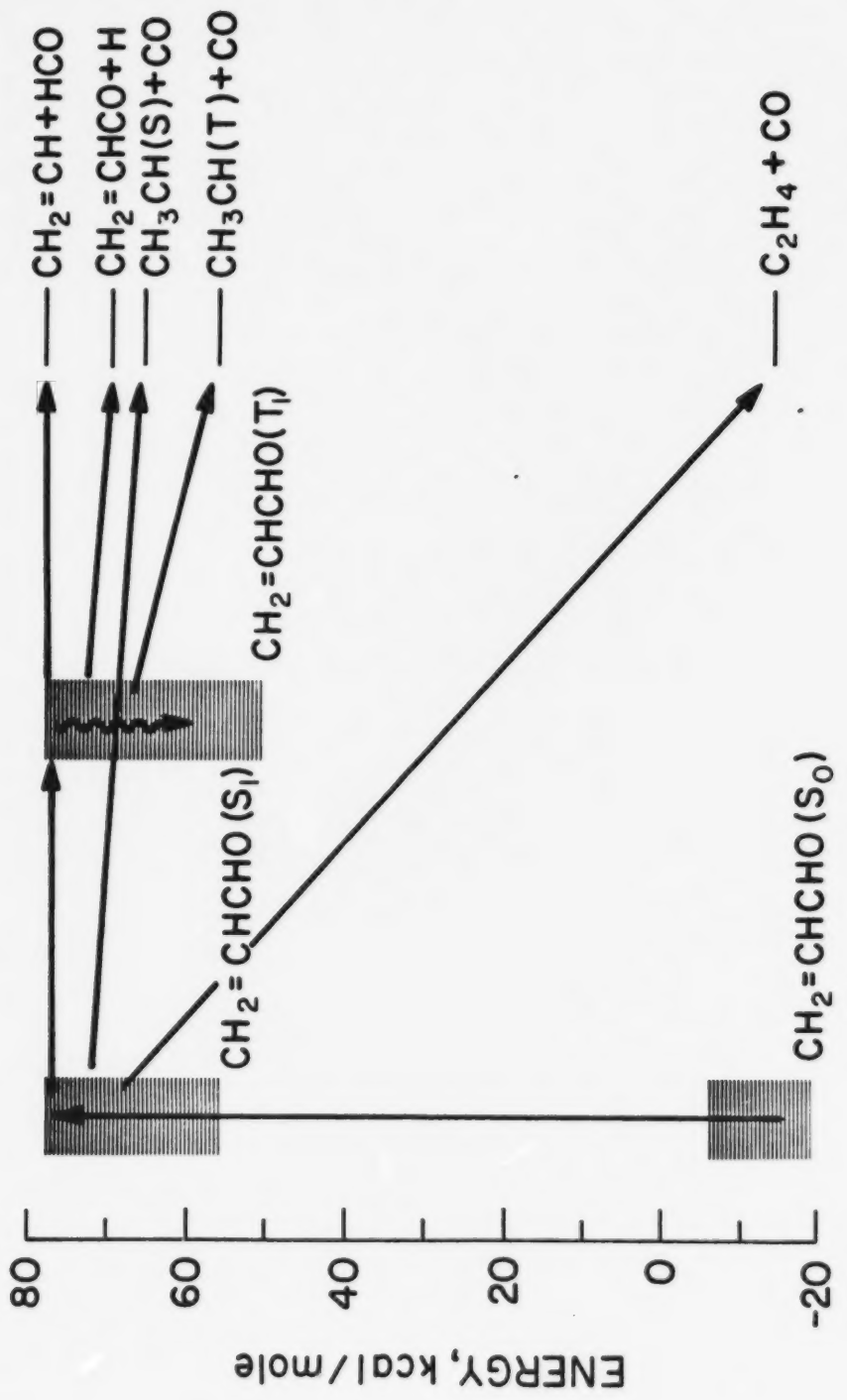

Figure 11. Summary of the enthalpy relationships among the various electronic states of the acrolein molecule and the potential channels for reaction.

Evidence from the Present Investigation elucidating the Primary Processes of Acrolein Photolysis in Air

The thermochemical, kinetic, and structural properties of the products observed in the present study and their measured quantum yields, provide new evidence for evaluating the primary photodecomposition processes in acrolein photolysis. More specifically, for the first time a detailed investigation of acrolein photochemistry, focusing on high dilutions of reactant in air, has been performed which provides unique and quantitative information pertaining to the mechanism of its photooxidation. The major products, ethylene and carbon monoxide, are well understood in terms of the molecular elimination process (I):

$$CH_2{=}CHCHO^* \longrightarrow C_2H_4 + CO \qquad (I)$$

Since the quantum yields of ethylene and carbon monoxide are not quenched to zero for photolyses in mixtures with a large excess of air, it is probable that this process occurs from an excited singlet state, particularly for experiments employing high air pressures in which quenching of the excited triplet state should be very efficient; i.e., through collision with triplet O_2. The molecular fragmentation process (I) is analogous to that observed in the photolysis of the aliphatic aldehydes. In such cases, the transfer of the carbonyl hydrogen atom to the carbon atom adjacent to the carbonyl group occurs from the excited singlet state with relatively low efficiency for excitation at 3130 A, but with increasing efficiency at shorter wavelengths as the energy of the absorbed

quantum becomes greater. Accordingly, for aliphatic aldehydes, a saturated alkane and CO are the products:

$$RCHO(S_1) \rightarrow RH + CO$$

As indicated earlier in this report, Coomber and Pitts (1969) suggested that process (I) occurs partially from the first excited singlet state. Accordingly, since the reductions of the quantum yields of C_2H_4 and CO were approximately equivalent with the addition of piperylene, an efficient triplet quencher, the authors proposed that the molecular elimination of these species also occurs from the excited triplet state of acrolein. However, recalling that this process (9) requires a spin inversion for the overall reaction to occur from the excited triplet species and, therefore, is spin forbidden, i.e., improbable, one is encouraged to examine other sources of ethylene and carbon monoxide for conditions of low pressures of added air. It is clear from the summary of enthalpy relationships among the different electronic states and products of the primary processes, Figure 11, that reaction (IV) which is spin allowed from the excited triplet state, can be a source of CO and C_2H_4:

$$CH_2{=}CHCHO(T_1) \rightarrow CH_3CH(T) + CO \qquad (IV)$$

Under the experimental conditions employed by Coomber and Pitts, the CH_3CH species formed in process (IV) would rearrange rapidly to form the ethylene molecule; this will be explained in the context of the

present investigation later in the discussion. It is intuitively clear that both ethylene and carbon monoxide yields must be quenched equivalently by piperylene addition (as observed by Coomber and Pitts) if this process were important. Therefore, although one cannot exclude the occurrence of process (9) [i.e., from the triplet state], it is not required to explain the experimental results.

The formation of vinyl and formyl radicals (process II) in the photolysis of acrolein at 3130 A receives additional support from the present investigation.

$$CH_2{=}CHCHO^{*} \longrightarrow CH_2{=}CH + HCO \qquad (II)$$

It is exceedingly difficult to rationalize the formation of formaldehyde and glyoxal, observed in the photolysis of the employed acrolein - air mixtures, without invoking the presence of the vinyl radical. Although previous studies delineating the reactions of the vinyl radical with oxygen are unknown to these authors, it is probable by analogy with the established reactions of simple alkyl radicals that the following processes are important:

$$CH_2{=}CH + O_2 \longrightarrow CH_2{=}CHOO \qquad (12)$$

$$CH_2{=}CHOO \longrightarrow \begin{array}{c} O\text{---}O \\ | \quad | \\ CH_2\text{---}CH \end{array} \longrightarrow OCH_2CHO \qquad (13)$$

$$OCH_2CHO \longrightarrow CH_2O + HCO \quad (HCO + O_2 \longrightarrow HO_2 + CO) \qquad (14)$$

$$OCH_2CHO + O_2 \longrightarrow HCOCHO + HO_2 \qquad (15)$$

If reactions (14) and (15) are the origins of formaldehyde and

glyoxal, respectively, then one would expect the formaldehyde to glyoxal ratio to vary in direct proportion to increasing oxygen pressures over a series of experiments. As demonstrated in Figure 12, this expectation is realized experimentally. Within the error of analysis for glyoxal and formaldehyde, the ratio [glyoxal]/[CH_2O] regressed against [O_2] follows a linear relationship which passes through the origin as expected in theory if reactions (14) and (15) are in fact the major processes leading to formaldehyde and glyoxal. Moreover, the slope of the line, approximately 1.1 x 10^{-18} cm^3 $molec^{-1}$, represents the first estimate of the rate coefficient ratio, k_{15}/k_{14}. The rate coefficient ratio for the analogous reactions (16) and (17) has been estimated by Niki and coworkers (1981) to be 5.4 x 10^{-20} cm^3 $molec^{-1}$ s^{-1}:

$$HOCH_2CH_2O \rightarrow CH_2O + CH_2OH \qquad (16)$$

$$HOCH_2CH_2O + O_2 \rightarrow HOCH_2CHO + HO_2 \qquad (17)$$

The results of the present study are in agreement with the observation that the beta-hydroxy alkoxy radicals represented in processes (16) and (17) are significantly more reactive toward decomposition than are other known alkoxy radicals (Niki, Maker, Savage, and Brietenback, 1978, 1981). However, the OCH_2CHO radical, considered in reactions 13-15, has a much greater tendency for decomposition relative to reaction with O_2 than has the simple alkoxy radicals. Nevertheless, the ratio of the two processes, (14) and (15), is still a factor of 10^{-2} of that observed for the $HOCH_2CH_2O$ radical.

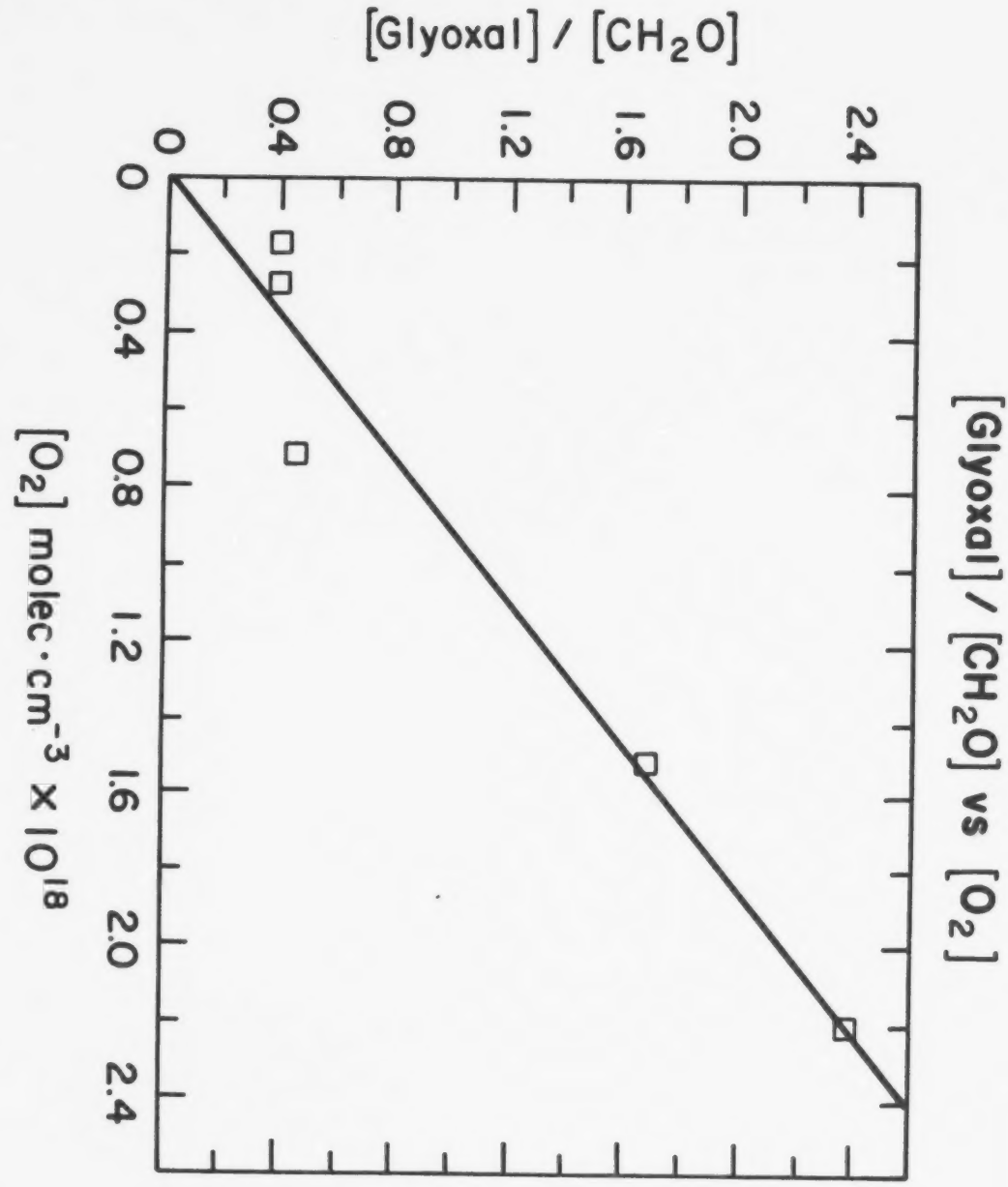

Figure 12. Regression of the ratio [HCOCHO]/[CH_2O] against [O_2] for 3130 Å photolysis of acrolein in air.

It is apparent from Figure 11, that the energy of an acrolein molecule excited at 3130 A is barely sufficient to permit dissociation from the upper, first populated, vibrational levels. We conclude, therefore, that dissociation of the excited singlet state by process (II) must occur before significant vibrational relaxation has taken place. Conceivably, intersystem crossing to the triplet manifold followed by decomposition via (II) from the triplet state may also occur provided that the S_1 to T_1 conversion is extremely rapid.

In the current investigation, the presence of product species to which the vinyl radical is a precursor does not provide unique evidence for the occurrence of process (II) since, alternatively, the primary process (V) could be a source of this radical in subsequent reactions. However, as will be explained, the occurrence of process (II) is required to elucidate other features of the product distribution which process (V) can not provide exclusively.

As already indicated, the studies of Umstead et al. (1978), Shinohara and Nichi (1982), and Fujimoto et al. (1985) provide substantial evidence that acrolein, promoted to the $S_2(pi,pi^*)$ state by absorption of short wavelength (<2000 A) light, decays via process (11) to form CH_3CH radicals and CO:

$$CH_2{=}CHCHO + h\nu \rightarrow (CH_3CH{=}C{=}O) \rightarrow CH_3CH + CO \qquad (11)$$

From a consideration of the thermochemistry, see Figure 11, it is apparent that even at 3130 A there is sufficient energy of

excitation for this process to occur. Accordingly, the evidence provided in the present work supports the occurrence of both primary processes (III) and (IV), as more specific expressions of (11):

$$CH_2{=}CHCHO + h\nu \longrightarrow CH_3CH(\text{Singlet}) + CO \qquad \text{(III)}$$

$$\longrightarrow CH_3CH(\text{Triplet}) + CO \qquad \text{(IV)}$$

Specifically, the appearance of the CH_3OH and CO_2 products in the amounts observed in the experiments reported here requires consideration of these processes.

In theory, formation of CO_2 and CH_3OH could arise from one or several of the following reactions:

$$CH_3CH + O_2 \longrightarrow (CH_3CHOO) \longrightarrow CH_3CO_2H^* \qquad (18)$$

$$CH_3CO_2H^* \longrightarrow CO_2 + CH_4 \qquad (19)$$

$$\longrightarrow CH_3 + CO_2H \ (CH_3O_2 + HO_2 + CO_2) \qquad (20)$$

$$\longrightarrow CH_3OH + CO \qquad (21)$$

$$CH_3CO_2H^* + M \longrightarrow CH_3CO_2H + M \qquad (22)$$

It is known from theoretical (t) and experimental (e) studies that the lifetime of the CH_3CH species is so finite that it is exceedingly difficult to obtain direct, empirical evidence for its existence; t: Nobes, Random, and Rodwell, 1980; Kyba, 1977; Harding, 1981; Altmann, Csizmadia, and Yates, 1974, 1975; e: Chong and Kistiakowsky, 1964; Su and Thornton, 1978. Under oxygen-free conditions, for example, it rearranges to form a highly excited ethylene molecule:

$$CH_3CH \longrightarrow CH_2CH_2^* \qquad (23)$$

Accordingly, the vibrationally enriched ethylene formed in (23) may disassociate (24) into acetylene and hydrogen molecules or be collisionally relaxed in (25):

$$CH_2CH_2^* \longrightarrow C_2H_2 + H_2 \qquad (24)$$

$$CH_2CH_2^* + M \longrightarrow CH_2CH_2 + M \qquad (25)$$

Ethylene and hydrogen are indeed trace products in the present investigation, which is in accord with our anticipation that, for our conditions of relatively high pressure of added air, collisional relaxation in (25) should follow reaction (23) with few exceptions. In addition, the results of this study suggest that rearrangement of the CH_3CH species, reaction (23), is more important (by 72%) than reaction with O_2 for the lowest pressure of oxygen employed (5.1 torr). Conversely, at one atmosphere of air, only 10% of the reaction of the CH_3CH radical takes place via channel (23).

Additional evidence for the formation of the CH_3CH radical, and hence, for the occurrence of reactions (III) and (IV), is the presence of methane among the products. The only conceivable channel for CH_4 formation in our system is via reaction (19) which presupposes the formation of the $CH_3CO_2H^*$ species in (18) for which, the CH_3CH radical, formed in processes (III) and (IV) is the precursor. In contrast, reaction (19) cannot be the only source of CO_2, in as much as the product ratio CH_4/CO_2 is much less than the value of unity required if CO_2 originates via (19) exclusively.

Reaction (20) indeed represents another source of CO_2 but the amount that can be rationalized via this channel is still insufficient to explain a CH_4/CO_2 ratio much greater than unity. As will be discussed in the following paragraph, an alternative source of CO_2 can be rationalized through the primary process (V). Another reaction pathway for the $CH_3CO_2H^*$ species is process (21) which results in the formation of CH_3OH and CO. The observation of CH_3OH among the products supports the occurrence of this process, since the alternative, disproportionation (26) of CH_3O_2 radicals formed in (20),

$$2CH_3O_2 \text{ --> } CH_3OH + CH_2O + O_2 \qquad (26)$$

which in principle could be a source of CH_3OH, has been demonstrated to be relatively unimportant in simulations employing the rates and reaction schemes appropriate for our experimental conditions. If in our evaluation, we can infer the unimportance of (26) in the experiments performed, then it is reasonable to conclude that process (21) may be the major source of the CH_3OH product.

As already indicated, a major source of CO_2 is required in addition to the reactions (19) and (20). A clue to the alternative origin of this product is perceived by noting that the ratio of CO_2 to glyoxal (HCOCHO) varies in the range of 1.9 at low pressures to near unity at the highest pressure of added air for which product data are available (360 torr); see Figure 13. Such a trend is consistent with the distribution expected following the primary process (V):

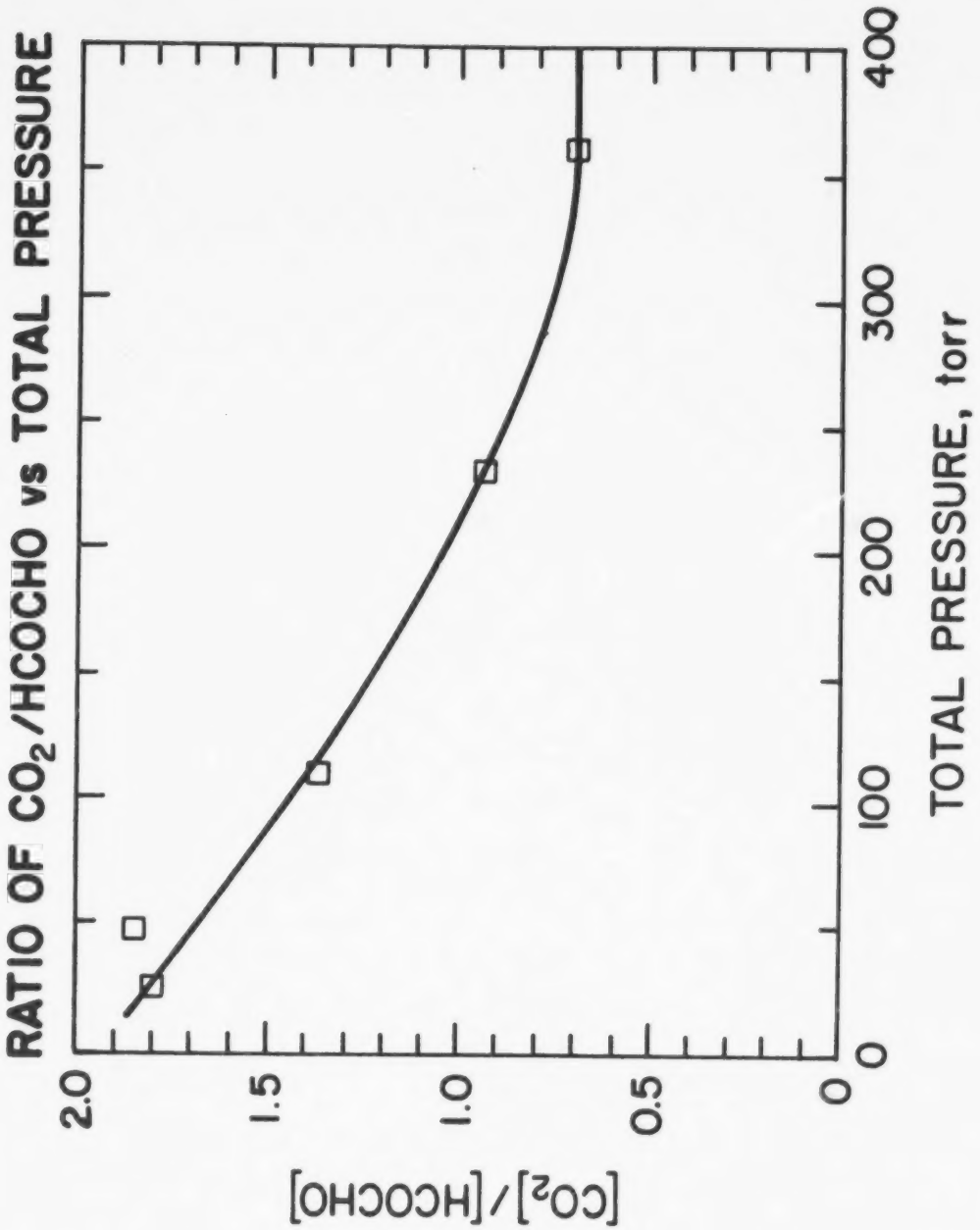

Figure 13. Ratio of CO_2 to glyoxol (HCOCHO) vs pressure of added air for photolysis of acrolein at 3130 Å.

$$CH_2{=}CHCHO^* \rightarrow CH_2{=}CHCO + H \ (CH_2{=}CHCOO_2 + HO_2) \qquad (V)$$

$$CH_2{=}CHCOO_2 + CH_2{=}CHCOO_2 \rightarrow 2CH_2{=}CH + 2CO_2 + O_2 \qquad (27)$$

$$CH_2{=}CH + O_2 \rightarrow OCH_2CHO \rightarrow HCOCHO, \text{ etc.} \qquad (12\text{-}15)$$

Furthermore, the occurrence of primary process (V) provides for the observed product imbalance with the measured amount of acrolein lost. In addition to the association of two $CH_2{=}CHCOO_2$ radicals in process (27), it is reasonable to anticipate the reaction of this species with the HO_2 radical as well:

$$CH_2{=}CHCOO_2 + HO_2 \rightarrow CH_2{=}CHCOO_2H + O_2 \qquad (28)$$

However, the employed analytical methods do not permit the detection of the product, peroxyacrylic acid.

Although the evidence for process (V) is indirect, it provides the attributes necessary to reconcile the quantum yield data for CO_2 with that of the other products; i.e., these data cannot be reconciled without its inclusion in the mechanism. The failure of other investigators to invoke this process in the direct photolysis of acrolein at 3130 A is the consequence of the less complete product analyses which characterized the previous work. Accordingly, the small but real H_2 product, observed in previous studies conducted in the absence of oxygen, could have been the result of abstraction (29) of atomic hydrogen from the excess acrolein reactant by H-atoms produced in reaction (V):

$$CH_2{=}CHCHO + H \rightarrow CH_2{=}CHCO + H_2 \qquad (29)$$

Coomber and Pitts (1969) reported a small amount of CO_2 product in their study of the photolysis of pure acrolein at 3130 A. Although they attributed this to a dark, wall reaction, it is conceivable that this product was the result of the reaction of CH_2=CHCO radicals formed in (V) with trace concentrations of O_2 present in their system.

Computer Simulation of Product Quantum Yields in the 3130 A Photolysis of Acrolein in Air

The NCAR CHEMSIM (1985) program was employed to simulate the complex chemistry which occurs in the acrolein system. The reactions included in the simulation are summarized in Table 6. Although the absolute values of the rate coefficients for many of these reactions are not known, the ratio of the rate constants which determine the various competitive pathways has been estimated via a numerical fit of the experimental data. Accordingly, an arbitrary yet reasonable value is chosen for one of the rate constants, usually for the A + M or A + O_2 reaction, to serve as a reference in the calculation. The parameters for CH_2O photolysis in the system (absorption cross section, and primary quantum yields) were derived from the previous studies of this substance (Horowitz and Calvert, 1978). The apparent first order rate coefficient employed for the photolytic reactions of CH_2O were estimated from the following relation:

$$k_x = (k_a)\ (\sigma_f/\sigma_a)\ (\phi_f/\phi_a),$$

Table 6

PROPOSED REACTION MECHANISM FOR ACROLEIN PHOTOLYSIS IN AIR AT 3130 A

(A)	CH_2=CHCHO + hv --> S_1	I_a, absorbed light intensity (quanta cm^{-3} s^{-1})
(I)	S_1 --> C_2H_4 + CO	$I_a\phi_I/[A] = 0.00177I_a/[A]$ $[A]^I$= initial acrolein concentration
(II)	S_1 --> CH_2=CH + HCO	
	(OCH_2CHO + HO_2 + CO)	$I_a\phi_{II}/[A] = 0.00102I_a/[A]$
(III)	S_1 --> T_1	$I_a\phi_{III}/[A] = 0.995I_a/[A]$
(IV)	S_1 --> CH_2=CHCHO + H	
	(CH_2=$CHCOO_2$ + HO_2)	$I_a\phi_{IV}/[A] = 0.000887I_a/[A]$
(V)	S_1 --> CH_3CH +CO	$I_a\phi_V/[A] = 0.000887I_a/[A]$
(14)	OCH_2CHO --> CH_2O + CO + HO_2	3.67×10^3
(15)	OCH_2CHO + O_2 --> HCOCHO + HO_2	7.9×10^{-15}
(VI)	T_1 --> CH_2=CH + CHO	
	(OCH_2CHO + HO_2 + CO)	1.28×10^5
(VII)	T_1 --> CH_3CH + CO	2.10×10^5
(VIII)	T_1 --> CH_2=CHCO + H	
	(CH_2CHCOO_2 + HO_2)	3.15×10^5
(IX)	T_1 + M --> CH_2=CHCHO + M	3.30×10^{-11}
(23)	CH_3CH --> CH_2=CH_2*	2.12×10^6
(18)	CH_3CH + O_2 --> (CH_3CHOO) --> CH_3CO_2H*	5.00×10^{-12}
(24)	CH_2=CH_2* --> C_2H_2 + H_2	1.00×10^6
(25)	CH_2=CH_2* + M --> CH_2=CH_2 + M	2.6×10^{-10}

Table 6 (continued)

(19)	$CH_3CO_2H^* \rightarrow CO_2 + CH_4$	4.84×10^4
(20)	$CH_3CO_2H^* \rightarrow CH_3 + CO_2H$	
	$(CH_3O_2 + HO_2 + CO_2)$	8.74×10^5
(21)	$CH_3CO_2H^* \rightarrow CH_3OH + CO$	9.02×10^5
(22)	$CH_3CO_2H^* + M \rightarrow CH_3CO_2H + M$	2.47×10^{-12}
(30)	$HCOCHO + h\nu \rightarrow CO + CH_2O$	see text
(32)	$HCOCHO + h\nu \rightarrow HCOH + CO$	
	$(HCOO_2H^* + CO)$	see text
(33)	$HCOO_2H^* \rightarrow CO_2 + H_2O$	1.00×10^6
(34)	$HCOO_2H^* + M \rightarrow HCOO_2H + M$	2.33×10^{-14}
(35)	$CH_2O + h\nu \rightarrow H_2 + CO$	see text
(36)	$CH_2O + h\nu \rightarrow H + HCO$	
	$(2HO_2 + CO)$	see text
(37)	$2HO_2 \rightarrow H_2O_2 + O_2$	3.00×10^{-12}
(38)	$2CH_3O_2 \rightarrow 2CH_3O + O_2$	1.17×10^{-13}
(39)	$2CH_3O_2 \rightarrow CH_3OH + CH_2O + O_2$	2.17×10^{-13}
(40)	$CH_3O + O_2 \rightarrow HO_2 + CH_2O$	1.30×10^{-15}
(41)	$CH_3O_2 + HO_2 \rightarrow CH_3O_2H + O_2$	1.50×10^{-12}
(42)	$2CH_2{=}CHCOO_2 \rightarrow 2CH_2{=}CH + 2CO_2 + O_2$	
	$(2OCH_2CHO + 2CO_2 + O_2)$	1.10×10^{-15}
(43)	$CH_2{=}CHCOO_2 + HO_2 \rightarrow CH_2{=}CHCOO_2H + O_2$	1.30×10^{-14}
(44)	$CH_2{=}CHCOO_2 + CH_3O_2 \rightarrow CH_2{=}CH + CO_2 +$	
	$CH_3O + O_2$ $(OCH_2CHO + CO_2 + CH_3O + O_2)$	3.60×10^{-14}

where k_x and k_a represent the apparent first order rate coefficients (s^{-1}) for photodecomposition of formaldehyde by path x and acrolein via path a; σ_f and σ_a are the absorption cross sections (cm^2 $molec^{-1}$) for formaldehyde and acrolein at 3130 A; and ϕ_f and ϕ_a are the quantum yields for the processes of interest in formaldehyde and acrolein, respectively.

A similar calculation was performed for the product glyoxal, although in this case the necessary parameters were derived from much less reliable data (Calvert and Layne, 1953; Plum, Sanhueza, and Atkinson, 1983; Hepburn, Buss, Butler, and Lee, 1983; Osamura, Schaefer, Dupuis, and Lester, 1981). We have combined the data of Calvert and Layne (1953) and Hepburn et al. (1983) to estimate the quantum yields of processes (30)-(32) at zero pressure: 0.77, 0.15, and 0.08, respectively. The following approximate relation was derived to describe the quenching of glyoxal photodecomposition from [1] the data of Plum et al. (1983) for 1 atmosphere of air, [2] our data for 24 torr of air (ϕ_d = 0.52), and [3] an assumed quantum yield of unity for zero pressure of air:

$$1/\phi_d = 1 + (P_{air}, \text{torr})\ (0.044)$$

The photoabsorption cross section of glyoxal at 3130 A was measured in this investigation, and a value of 2.2×10^{-20} cm^2 $molec^{-1}$ was obtained. From these data and employing an expression analogous to that given previously for CH_2O (k_x), the apparent first order rate coefficients for glyoxal decomposition were calculated.

The rate coefficients for reactions (37) through (44) were

derived from the available literature (Gardner, Wijayaratne, and Calvert, 1984) and estimates based upon analogous, well known reactions.

Simulations were made in a first series of runs using the procedure outlined above for the estimation of the photolysis constants for formaldehyde and glyoxal. The calculated rate of loss of both formaldehyde and glyoxal appeared to be much greater than was observed in the experiments. Therefore, it is hypothesized that the small amounts of formaldehyde and glyoxal formed in the experiments were partially absorbed into the trace water product, existing as a film on the inside surface of the reaction vessel, to form stable hydrates of these species. If this were the case, then these compounds would be effectively transparent to the photolysis light and yet would be recovered efficiently by the techniques (see experimental procedure) employed in the product analysis. Adopting this hypothesis, simulations were performed employing rates of formaldehyde and glyoxal loss which were one hundredth of those used earlier. Since these simulations permitted an improved correlation of the product data, we conclude that this hypothesis is a reasonable simulacrum of the fates of formaldehyde and glyoxal in the reaction vessel.

The results of the simulations are shown in Figures 14-20. In each figure, the data representing the measured quantum yields are indicated by squares, while the simulated quantum yield data are designated by crosses. In view of the considerable complexity of the acrolein photochemical system, it is felt that the agreement between the experimental data and the simulations is reasonably

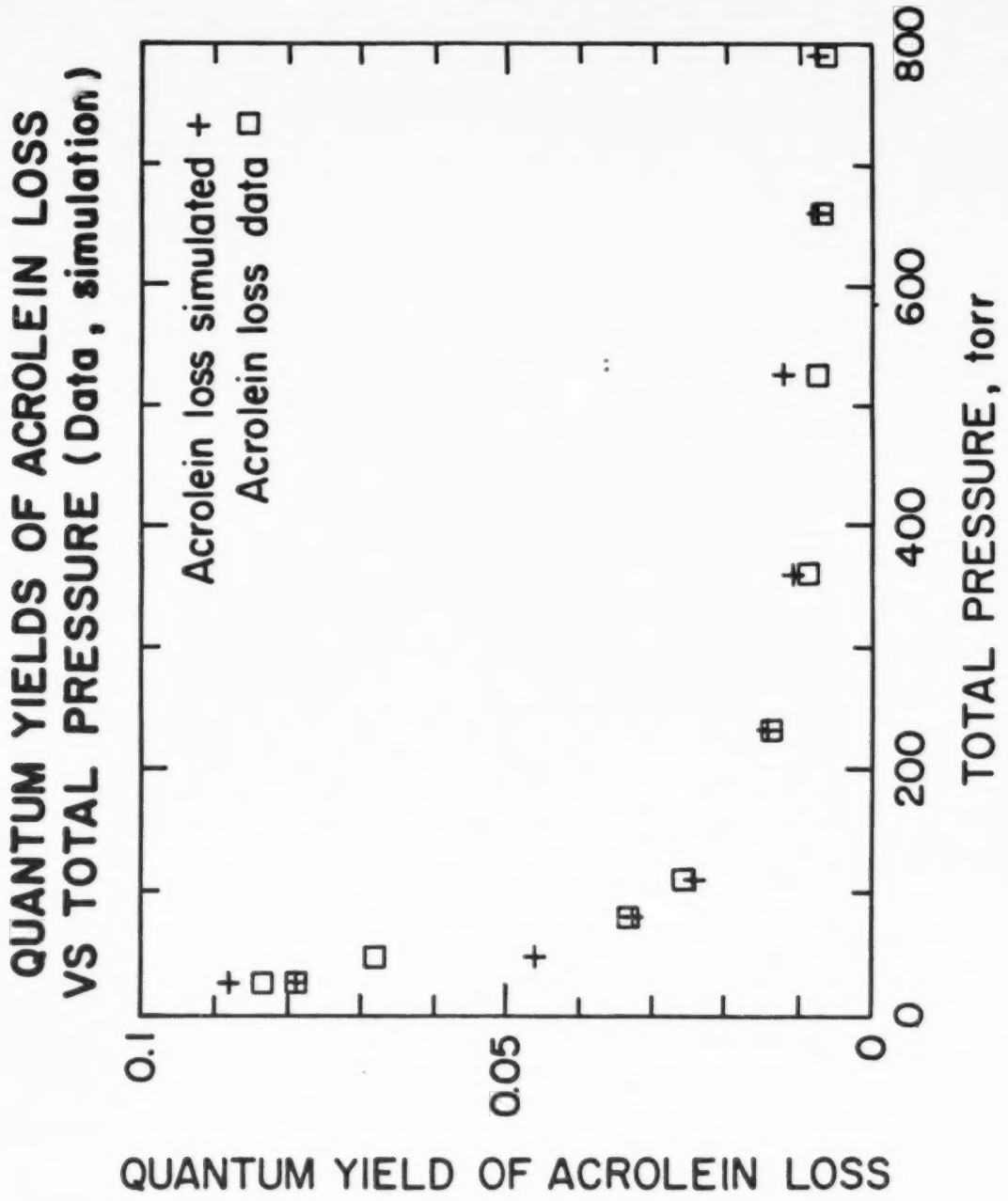

Figure 14. Comparison of simulated (crosses) and measured (squares) quantum yield of acrolein loss vs total pressure (torr) of reactant-air mixture.

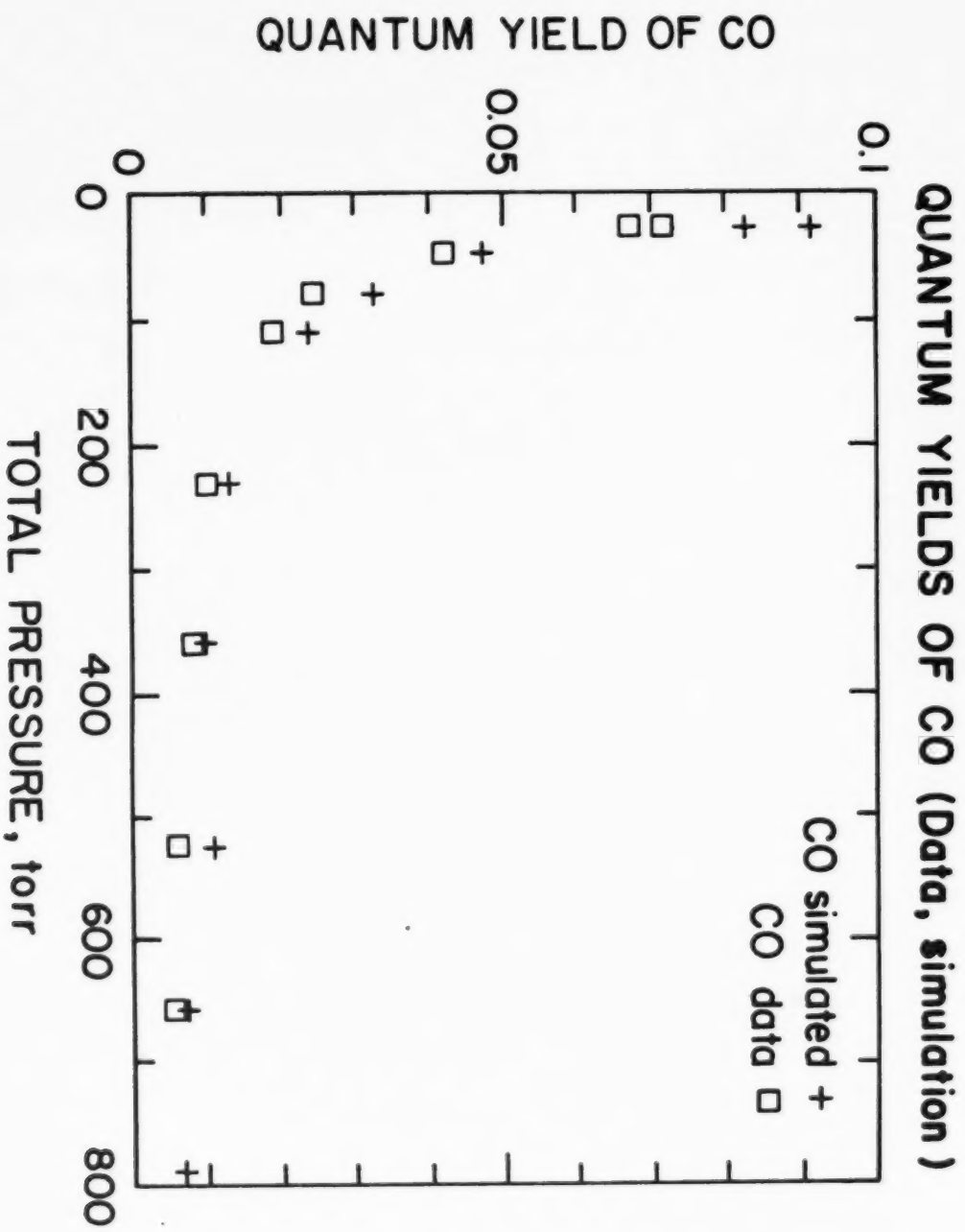

Figure 15. Comparison of simulated (crosses) and measured (squares) quantum yield of CO produced vs total pressure (torr) of reactant-air mixture.

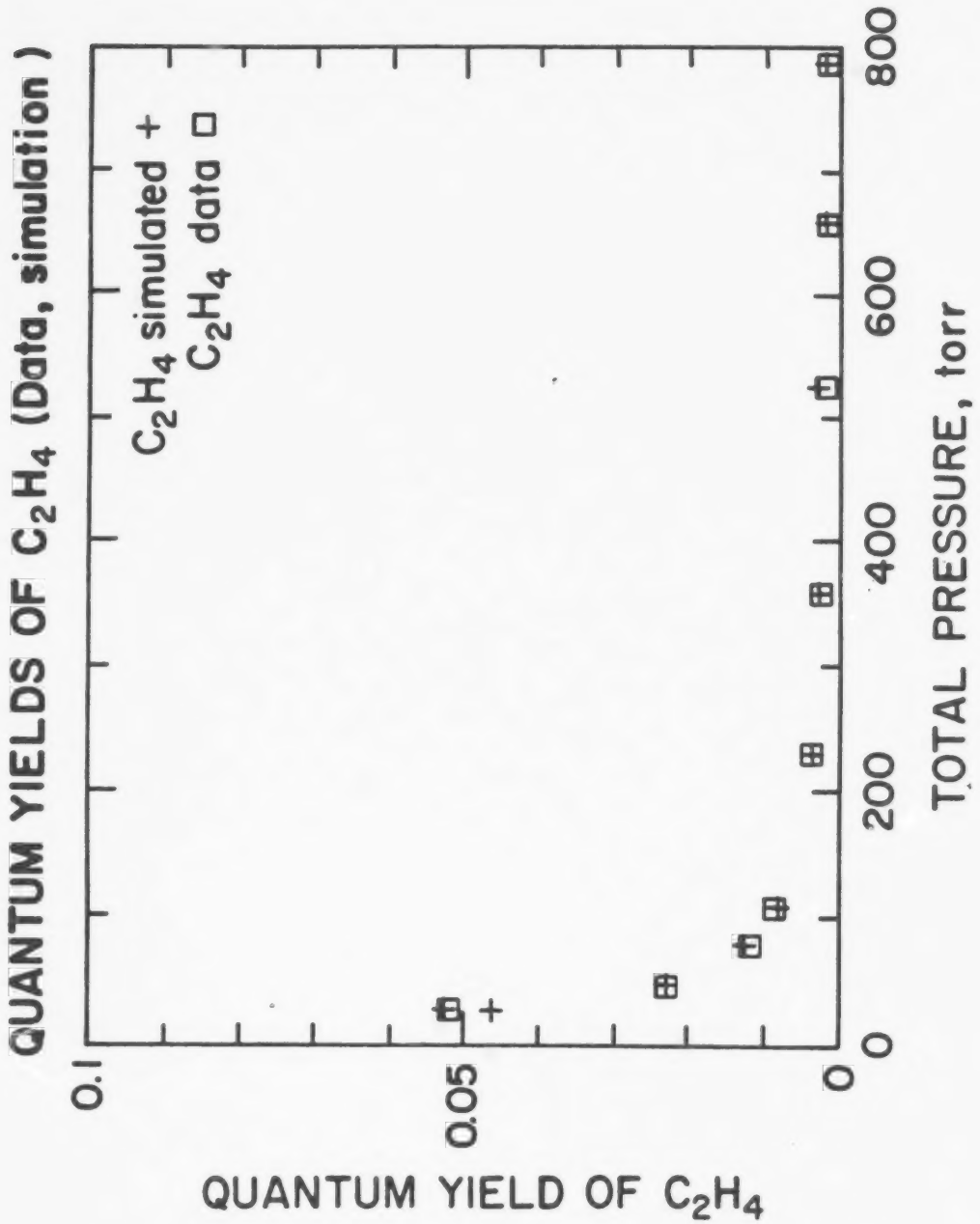

Figures 16. Comparison of simulated (crosses) and measured (squares) quantum yield of C_2H_4 vs total pressure (torr) of reactant-air mixture.

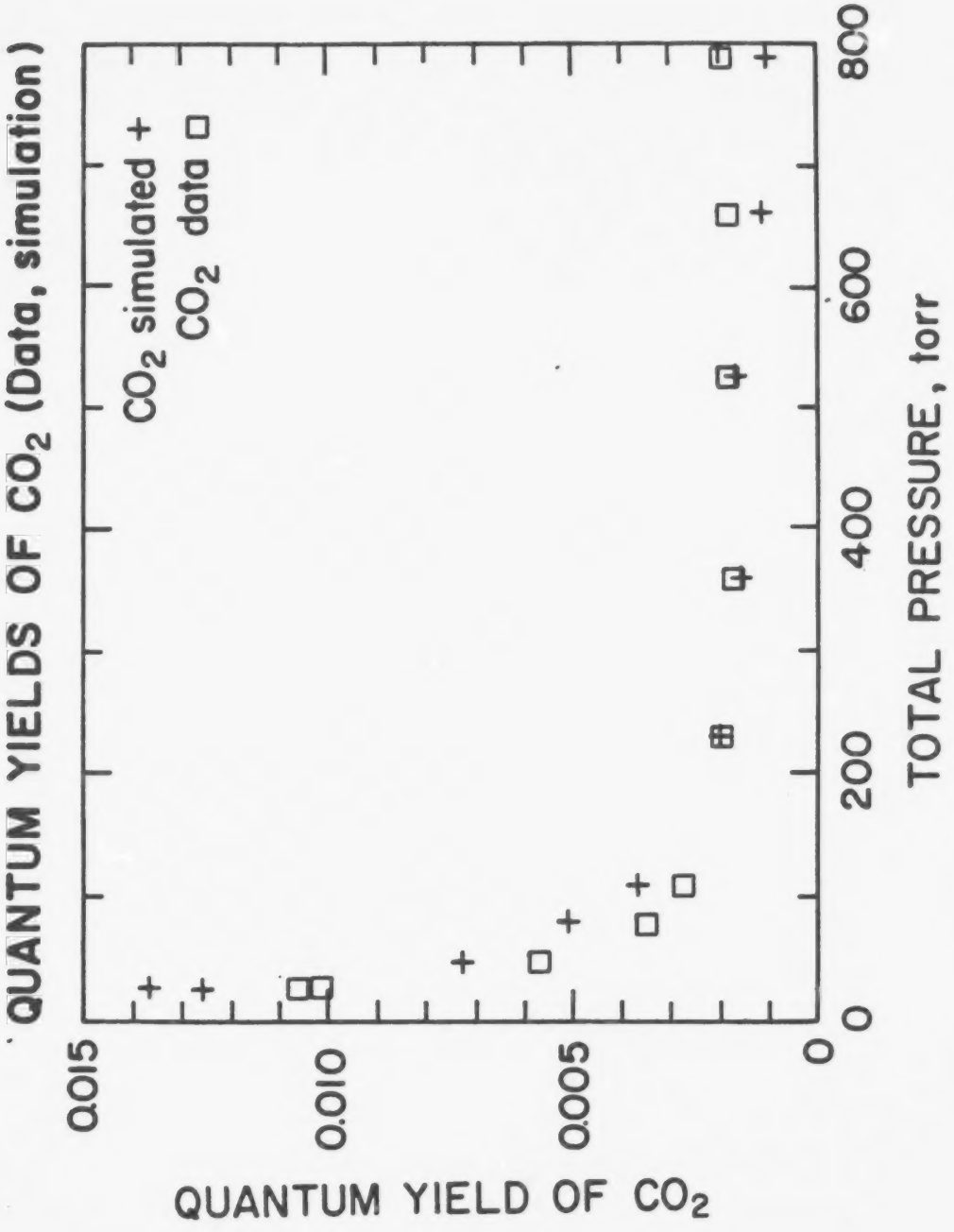

Figure 17. Comparison of simulated (crosses) and measured (squares) quantum yield of CO_2 vs total pressure (torr) of reactant-air mixture.

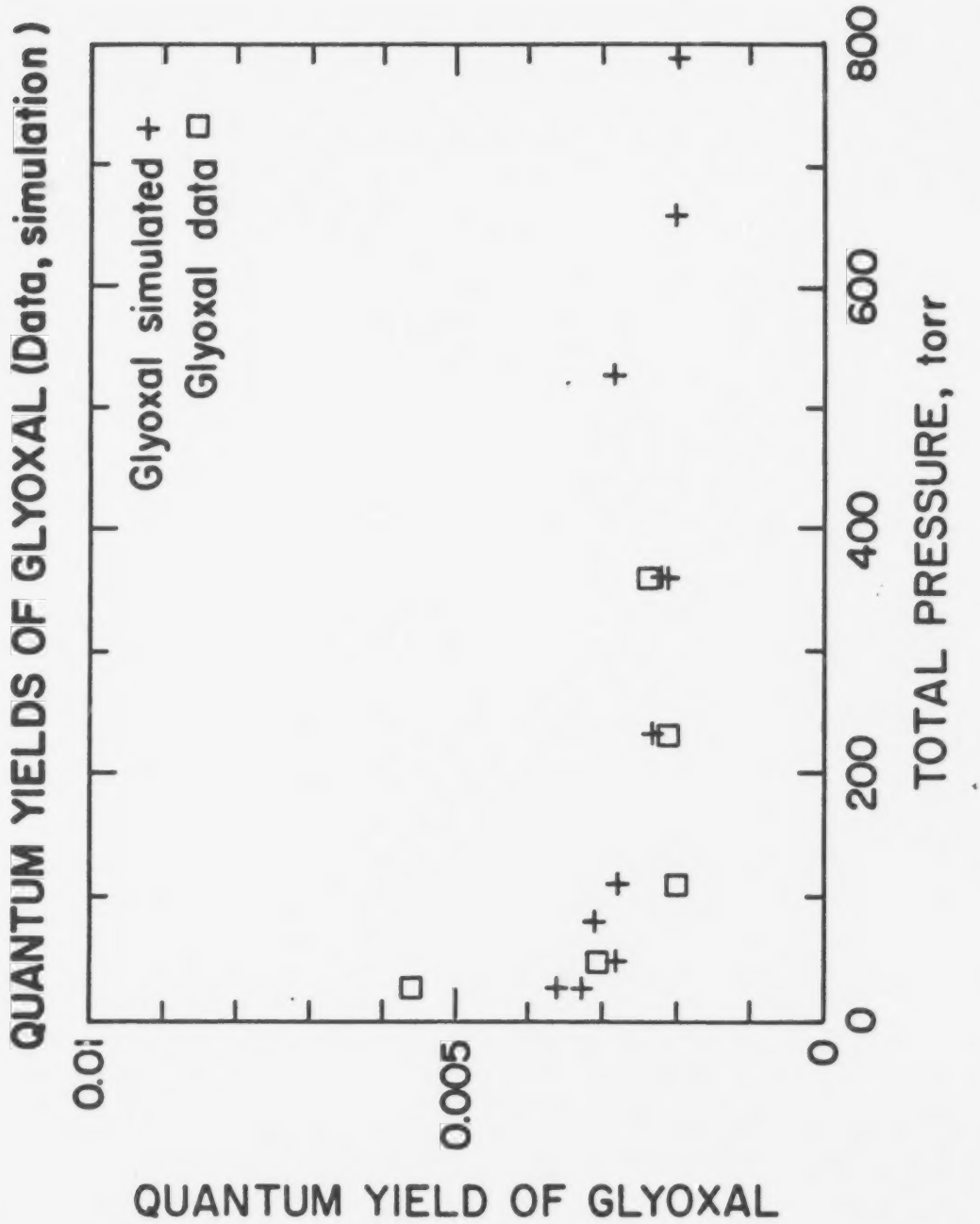

Figure 18. Comparison of simulated (crosses) and measured (squares) quantum yield of glyoxal vs total pressure (torr) of reactant-air mixture.

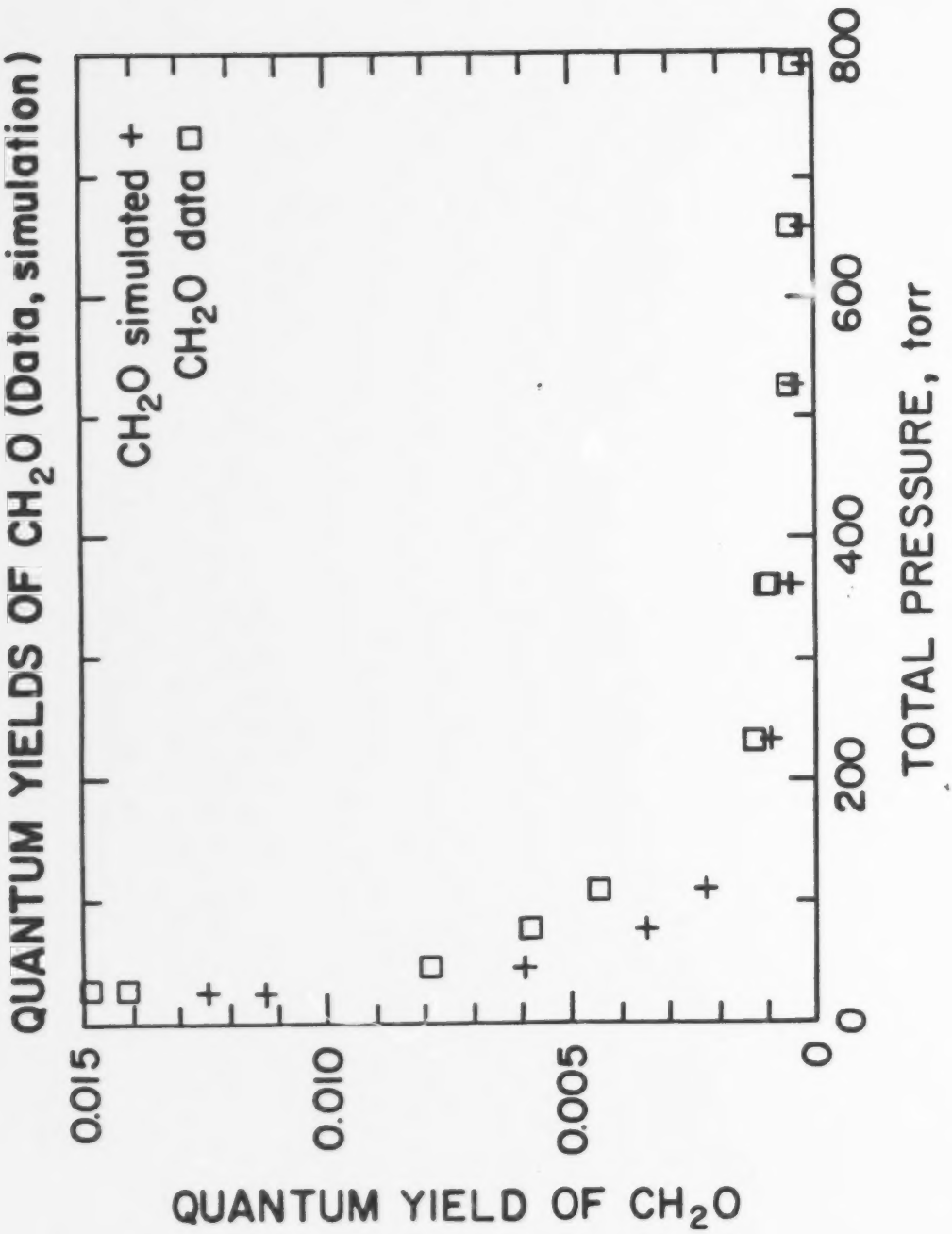

Figure 19. Comparison of simulated (crosses) and measured (squares) quantum yield of formladehyde vs total pressure (torr) of reactant-air mixture.

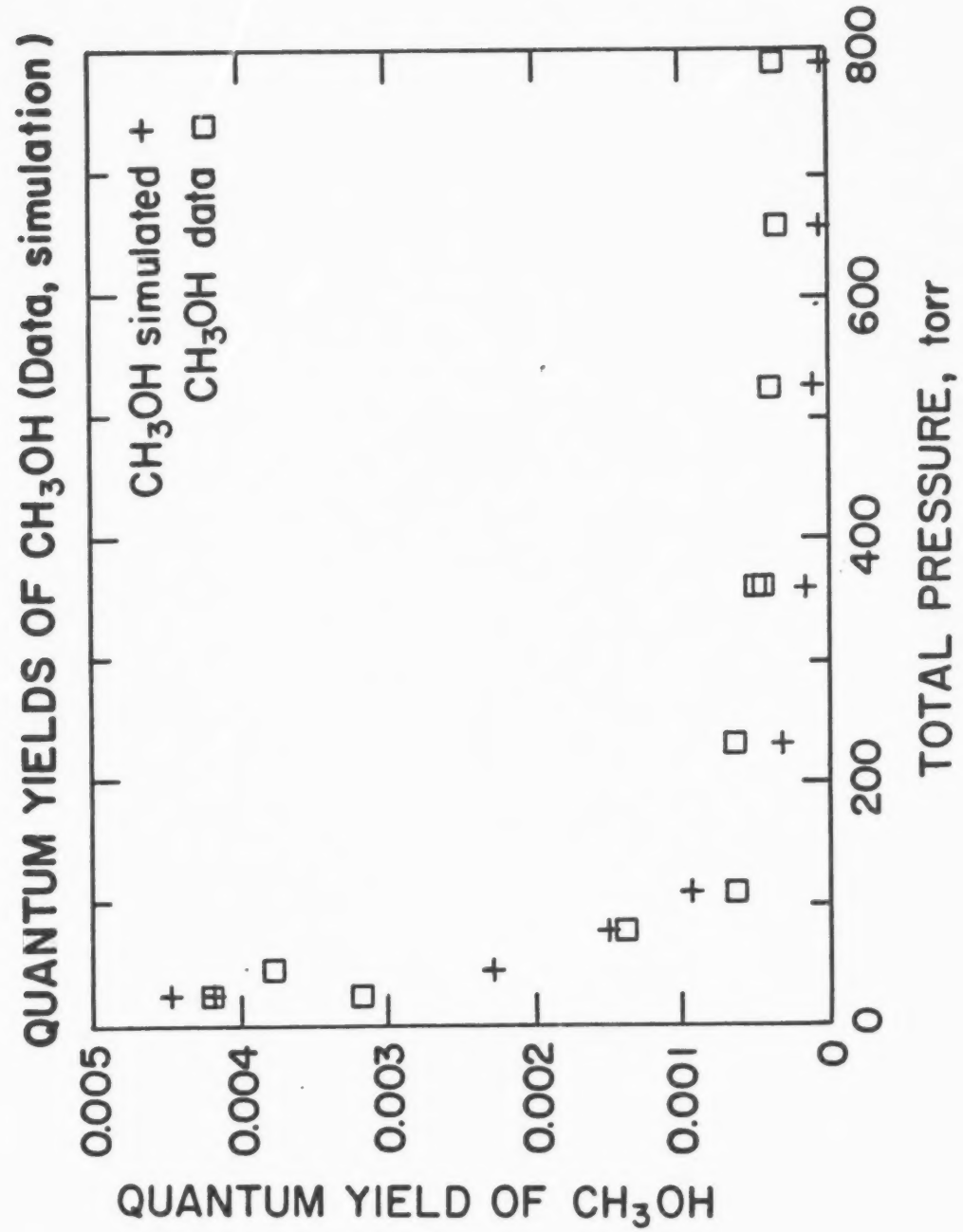

Figure 20. Comparison of simulated (crosses) and measured (squares) quantum yield of methanol vs total pressure (torr) of reactant-air mixture.

good, adding confidence to the interpretation of the mechanism given in this study.

The Apparent First Order Photolytic Rate Coefficient for the Decay of Acrolein in the Lower Troposphere

The product quantum yield data and the photoabsorption cross sections of acrolein presented in this investigation may be utilized to derive an estimate of the apparent first order rate coefficient (J) for the photodecomposition of acrolein in the lower troposphere as a function of solar zenith angle. Since, with only a few exceptions (not reported in this work) photochemical initiation was restricted to 3130 A, the wavelength dependence of the observed quantum yields is unknown at present. However, it is not improbable that the quantum yields may be insensitive to initiating wavelength of light for the energies of quanta available within the troposphere, as is the case for acetone (Gardner et al., 1984). Since the absorption spectrum of acrolein (see Figure 7) reveals some structure in the long wavelength region of its first absorption band, the lifetime of the excited state should be considerably longer at lower energies of excitation; i.e., the excited acrolein has more opportunity to be collisionally quenched to the ground state. Accordingly, one would expect the photodecomposition of acrolein to be much less efficient at wavelengths longer than 3130 A. In fact, some preliminary experiments at longer wavelengths have been performed as the basis for an extended evaluation of this work, and the results are in agreement with this expectation. In either

case, the assumption of invariance for the quantum yields vs wavelength is pragmatic in that it provides a maximum value of J. Hence, assuming that the 3130 A data presented in this work are representative of the other wavelengths within the acrolein absorption spectrum up to the atmospheric cut-off of radiation (2900 A), we may estimate maximum J values using the actinic flux estimates of Demerjian, Schere, and Peterson (1980) for the condition of zero surface albedo. These data, summarized in Table 7, are comparable to the values for acetaldehyde. At a solar zenith angle of 40 degrees, the photodissociation lifetime of acrolein in the troposphere is greater than 5 days. For comparison, the same calculation for acetone, acetaldehyde, and formaldehyde results in lifetimes of 14.8 days, 5.3 days, and 5.9 hours, respectively. If photodissociation were the only loss mechanism for acrolein in the troposphere, we would anticipate a reasonably long residence time in this region of the atmosphere. However, the measured rate coefficient for HO-radical attack on acrolein is large, $k = 1.9 \times 10^{-11}$ cm^3 $molec^{-1}$ s^{-1}. Therefore, assuming an average [HO] of approximately 10^6 molec cm^{-3}, the average lifetime of the acrolein molecule with respect to HO attack is only 14.6 hours. Obviously, the major loss mechanism for acrolein is through reaction with the HO-radical; i.e., the photochemical destruction of acrolein is relatively unimportant within the troposphere.

The quantum yields of acrolein loss observed in this investigation can be represented as a function of concentration of air ([M], molec cm^3) as expressed succinctly by the following equation:

Table 7

ESTIMATED MAXIMUM J VALUES
FOR ACROLEIN IN THE LOWER TROPOSPHERE

Solar Zenith Angle (degrees)	J (s^{-1})
0	2.8×10^{-6}
20	2.7×10^{-6}
40	2.3×10^{-6}
60	1.5×10^{-6}
78	0.37×10^{-6}
86	0.08×10^{-6}

$$1/(\phi_A - 0.00400) = 0.086 + 1.613 \times 10^{-17} \text{ [M]}$$

A marked increase in the photolytic rate of acrolein loss in the troposphere is anticipated with increasing altitude, i.e., lower pressures of air. From the simulations which have been conducted in the present study, the contribution (quantum yield) of each of the primary processes to the total decomposition of acrolein has been estimated for various pressures of air. These data, delineated in Figure 21, suggest that the ethylidene (CH_3CH) and CO forming reactions (III) and (IV) are the dominant processes for decomposition in acrolein photolysis under atmospheric conditions. Nevertheless, a significant fraction of acrolein decay occurs through other reaction channels. In particular, we suggest that in the lower troposphere, process (I) forming C_2H_4 and CO, is somewhat more important than CH_2=CHCO + H radical generation in (V) or vinyl and HCO radical formation in (II).

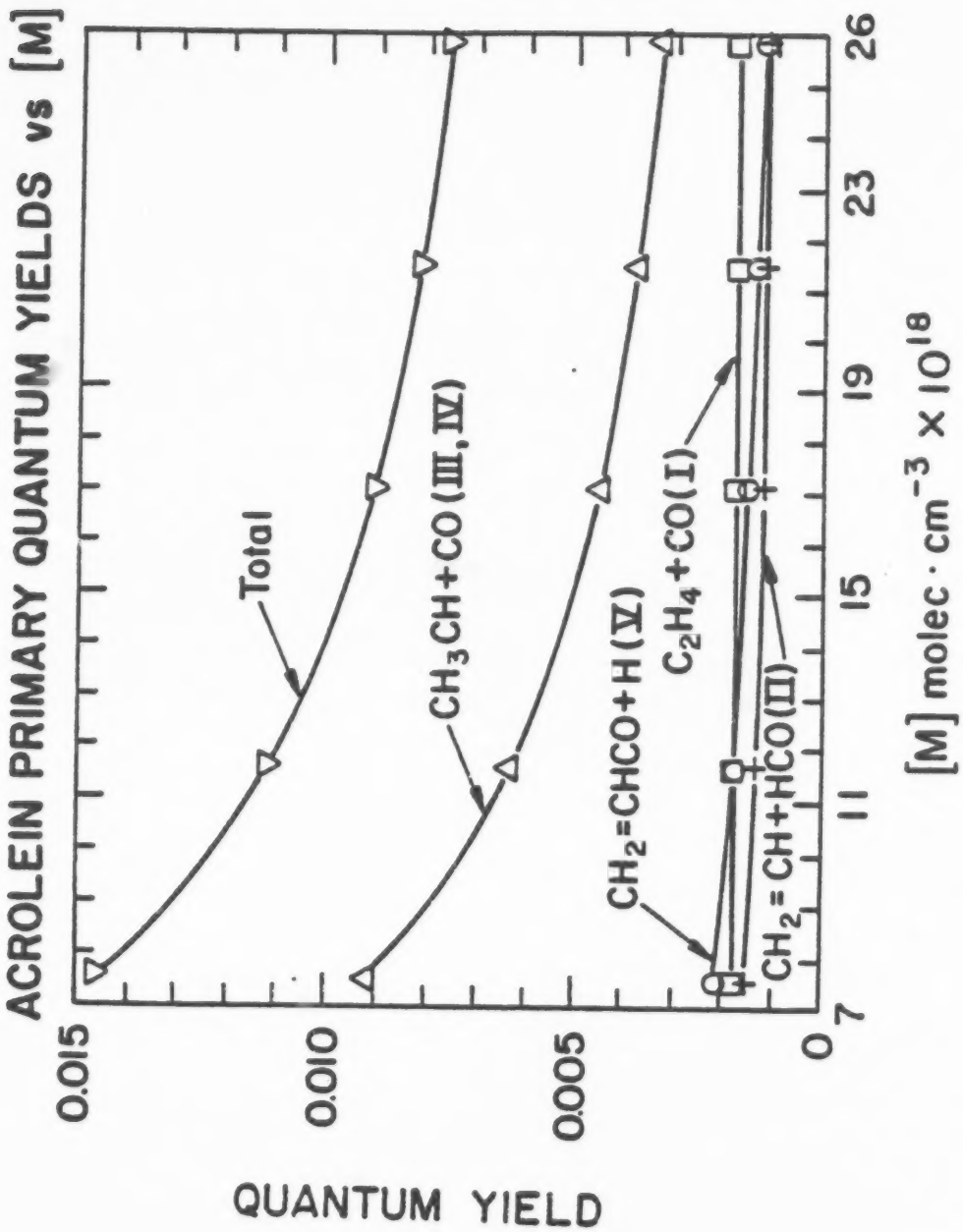

Figure 21. Contribution (quantum yield) of each of the primary processes to the total decomposition of acrolein at 3130 Å, as a function of total number of density (molecules cm^{-3}).

FOOTNOTES

1) For a recent review of the photochemistry of acrolein see: E. K. C. Lee and R. S. Lewis, "Photochemistry of Simple Aldehydes and Ketones in the Gas Phase," Adv. Photochem., 12, 1-95 (1980).

2) A grade of fused silica which has a better short-wavelength transmission than quartz, extending to approximately 160 nm (Spectra-Physics, Amersil, Inc.).

3) Commercially available under the name "Torr-seal" from Varian Associates, Vacuum Division, Palo Alto, California.

4) The metal O-ring joint incorporates a heat radiator (several circular blades) to dissipate the heat generated by the light source.

5) A full-scale difference of 0-100 mV, conveniently measured with a standard chart recorder, is obtained by placing a 100 ohm resistance across the recorder terminals; i.e., in series with two analog output.

6) Loschmidt's number is the number of molecules in one cubic centimeter of a gas at 1 atmosphere pressure (760 torr) and 0°C (1 cm^3 = 1 ml).

7) The expansion series is $e^x = 1 + x + x_2/2! + x^3/3! + \ldots$; since x is small $x^2/2!$ etc. may be neglected and the expansion becomes $e^x = 1 - \eta\sigma\ell$. Then $I_a = (1-e^{-\eta\sigma\ell})I_o$ becomes $I_o[1-1-\eta\sigma\ell)]$ which is simply $\eta\sigma\ell I_o$.

8) No contaminating substances were detected.

9) R. Renaud and L. C. Leitch, "Synthesis of 1, 2-dialkyl-hydrazines and the corresponding azoalkanes," Can. J. Chem., 32, 545-549 (1954).

10) P_s is the pressure (torr) of the gaseous sample in the sample chamber. x is the mole fraction of the component. V_s is the volume (0.07652 liter) of the sample chamber; V_p and V_{p+s} are the respective volumes (0.5725 and).6490 liter) of the gas piston and combined gas piston-sample chamber. R and T are the gas constant (8.2054×10^{-2} atm liter $mole^{-1}$ K^{-1}) and absolute temperature (Kelvins, K).

11) AU = area units of chromatographic trace as integrated by HP 339A computer/recorder.

12) Water is undoubtedly a secondary product (e.g., from H_2O_2) in the photooxidation of acrolein. However, it is an ubiquitous substance in glass systems, easily desorbed from the interior structure of the reaction cell through slow diffusional processes which may occur during a long experiment. The quantum yield of water product, although it must reflect some contribution from the photochemical mechanism, is determined largely by unknown contributions from trivial (glass wall) sources, unrelated to the homogeneous reactions of acrolein.

REFERENCES

Altmann, J. A., I. G. Csizmadia, and K. Yates, J. Amer. Chem. Soc., 96, 4196 (1974); ibid., 97, 5217 (1975).

Altshuller, A. P., and S. P. McPherson, Spectraphotometric analysis of aldehydes in the Los Angeles atmosphere, J. Air Poll. Contr. Assoc., 13, 109-111, 1963.

Atkinson, R., S. M. Aschmann, J. N. Pitts, Jr., Int. J. Chem. Kinet., 15, 75 (1983).

Aves, A. C. P., J. Christoffersen, and J. M. Hollas, Mol. Phys., 20, 625 (1971).

Becker, R. S., K. Inuzuka, and J. King, J. Chem. Phys., 52, 5164 (1970).

Benson, S. W., "Thermochemical Kinetics", John Wiley & Sons, N. Y. (1976).

Blacet, F. E., G. H. Fielding and J. G. Roof, J. Amer. Chem. Soc., 59, 2375 (1937).

Borden, W. T., and E. R. Davidson, Ann. Rev. Phys. Chem., 30, 125 (1979).

Brand, J. C. D., and D. G. Williamson, Discuss. Faraday Soc., 35, 184 (1963).

Calvert, J. G., and G. S. Layne, J. Amer. Chem. Soc., 75, 856 (1953).

Chong, D. P., and G. B. Kistiakowsky, J. Phys. Chem., 68, 1793 (1964).

Coomber, J. W., and J. N. Pitts, Jr., J. Amer. Chem. Soc., 91, 547 (1969).

Davidson, E. R., and L. E. Nitzche, J. Amer. Chem. Soc., 101, 6524 (1979).

Demerjian, K. L., K. L. Schere, and J. T. Peterson, Adv. Environ. Sci. Technol., 10, 369 (1980).

Dykstra, C. E., J. Amer. Chem. Soc., 98, 7182 (1976).

El-Sayed, M. A., J. Chem. Phys., 38, 2834 (1963); Acc. Chem. Res., 1, 8 (1968).

Fujimoto, G. T., M. E. Umstead, and M. C. Lin, J. Chem. Phys. Chem., 82, 3042 (1985).

Gardner, E. P., R. D. Wijayaratne, and J. G. Calvert, J. Phys. Chem., 88, 5069 (1984).

Graedel, T. E., "Chemical Compounds in the Atmosphere", Academic Press, N. Y. (1978).

Hansen, D. A., Ph.D. Thesis, University of California, Irvine (1973).

Hansen, D. A., and E. K. C. Lee, J. Amer. Chem. Soc., 95, 7900 (1973).

Harding, L. B., J. Amer. Chem. Soc., 103, 7439 (1981).

Harrison, A. G., and F. P. Lossing, Can. J. Chem., 37. 1696 (1959).

Hepburn, J. W., R. J. Buss, L. J. Butler, and Y. T. Lee, J. Phys. Chem., 87, 3638 (1983).

Horowitz, A., and J. G. Calvert, Int. J. Chem. Kinet., 10,805 (1978).

Horowitz, A., and J. G. Calvert, Int. J. Chem. Kinet., 10, 713 (1978).

Kato, T. and Y. Hanai, GC and GC-MS environmental analysis of photochemical smog component, Paper presented at 24th Lecture Meeting, Japan Soc. for Anal. Chem., (Saporo, Japan), Oct. 1-5, 1975 (APTIC No. 81207).

Kharasch, M. S., J. Res. Natl. Bur. Std., 2, 359-430 (1929).

Kyba, E. P., J. Amer. Chem. Soc., 99, 8330 (1977).

Lee, E. K. C., and R. S. Lewis, Adv. Photochem., 12, 1 (1980).

NCAR CHEMSIM program; developed at NCAR through the leadership of Steacie Walters, Atmospheric Chemistry Division, NCAR, Boulder, CO.

Niki, H., P. D. Maker, C. M. Savage and L. P. Breitenbach, Chem. Phys. Lett., 80, 499 (1981).

Niki, H., P. D. Maker, C. M. Savage and L. P. Brietenbach, J. Phys. Chem., 82, 135 (1978).

Nobes, R. H., L. Radom, and W. R. Rodwell, Chem. Phys. Lett., 74, 269 (1980).

Osamura, Y., H. F. Schaefer III, Michel Dupuis, and W. A. Lester, Jr., J. Chem. Phys., 75, 5828 (1981).

Osborne, A. D., J. N. Pitts, Jr., and E. R. Darley, Intern. J. Air Water Pollution, 6, 1 (1962).

Plum, C. N., E. Sanhueza, R. Atkinson, W. P. Carter, and J. N. Pitts, Jr., Environ. Sci. Technol., 17, 479 (1983).

Reid, R. C., J. M.Prausnitz, and T. K. Sherwood, "The Properties of Gases and Liquids", McGraw-Hill Book Company, N. Y. (1977).

Shinohara, H., and N. Nishi, J. Chem. Phys., 77, 234 (1982).

Stull, D. R., E. F. Westrum, Jr., and G. C. Sinke, "The Chemical Thermodynamics of Organic Compounds", John Wiley & Sons, Inc., N. Y. (1969).

Su, D. T. T., and E. R. Thornton, J. Amer. Chem. Soc., 100, 1972 (1978).

Thompson, H. W., and J. W. Linnett, J. Chem. Soc., 1452 (1935).

Umstead, M. E., R. G. Shortridge, and M. C. Lin, J. Phys. Chem., 82, 1455 (1978).

Weir, N. A., J. Chem. Soc., 6870 (1965).

APPENDIX

Supplemental Stern-Volmer plots of product yields for 3130 Å photolysis of acrolein in air at ~25° C.

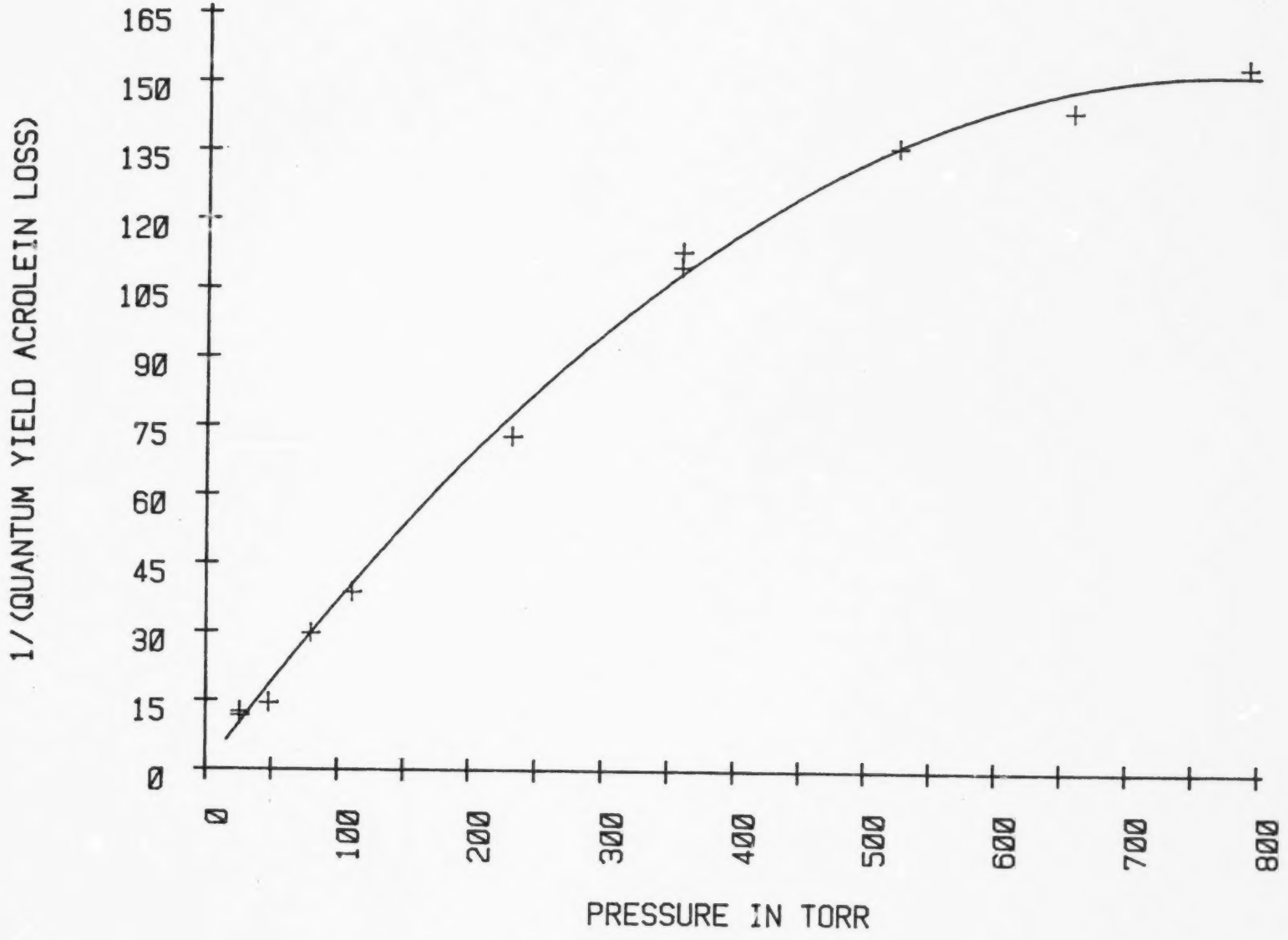
1/(QUANTUM YIELD ACROLEIN LOSS)
165
150
135
120
105
90
75
60
45
30
15
0
0
100
200
300
400
500
600
700
800
PRESSURE IN TORR

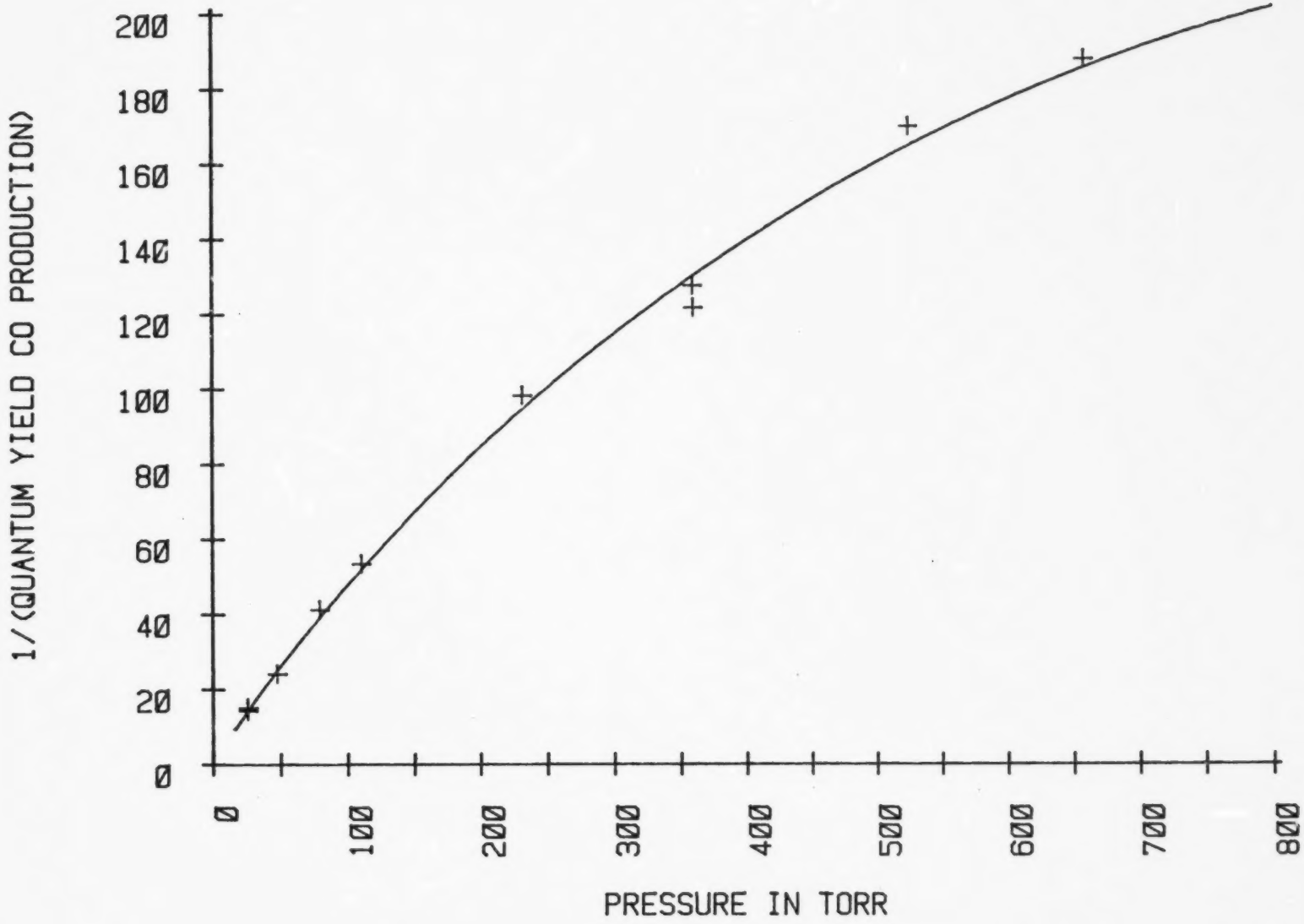
1/(QUANTUM YIELD CO PRODUCTION)
200
180
160
140
120
100
80
60
40
20
0
0
100
200
300
400
500
600
700
800
PRESSURE IN TORR

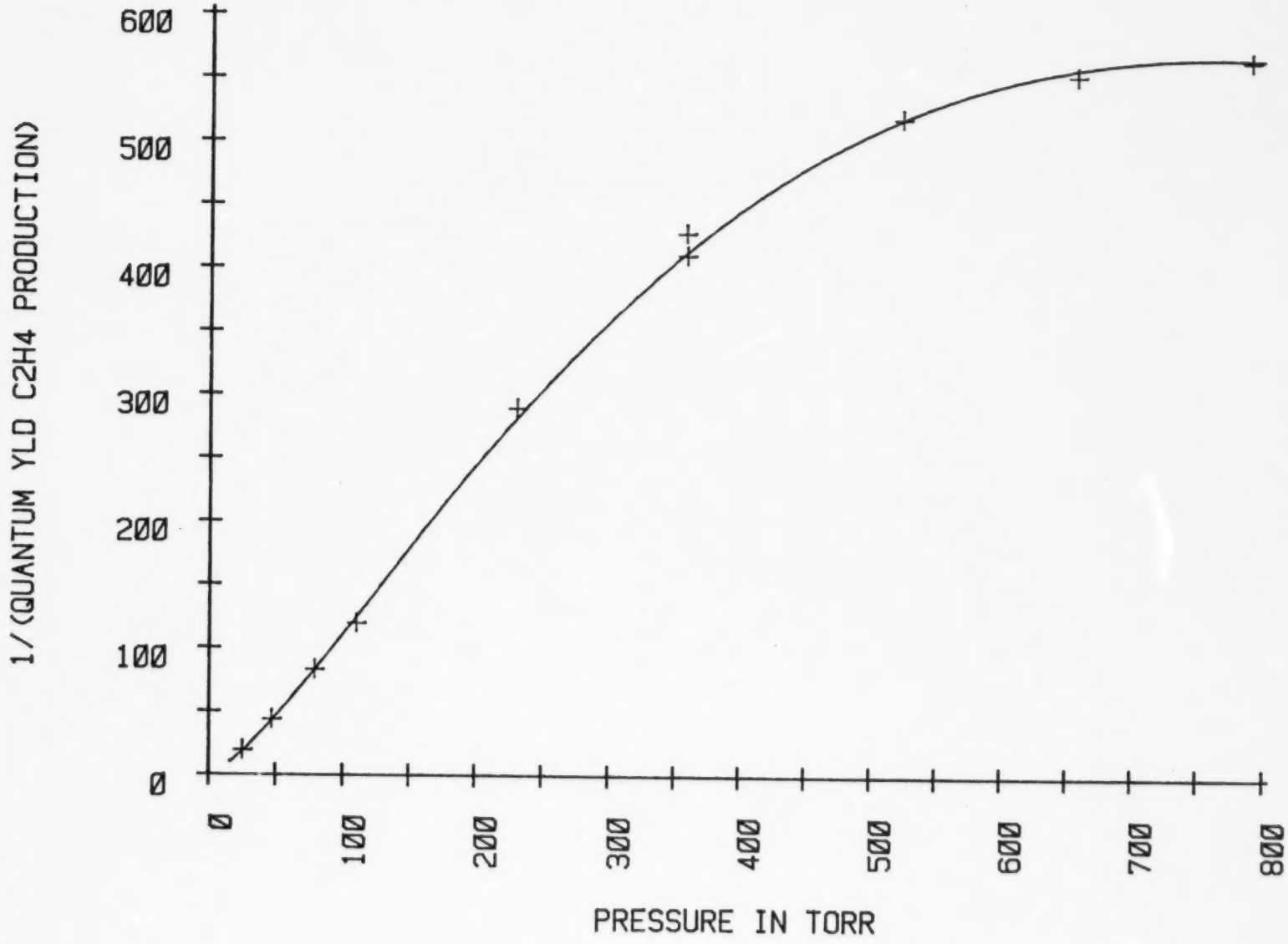
1/(QUANTUM YLD C2H4 PRODUCTION)
600
500
400
300
200
100
0
0
100
200
300
400
500
600
700
800
PRESSURE IN TORR

1/(QUANTUM YIELD CO2 PRODUCTION)
600
500
400
300
200
100
0
0
100
200
300
400
500
600
700
800
PRESSURE IN TORR

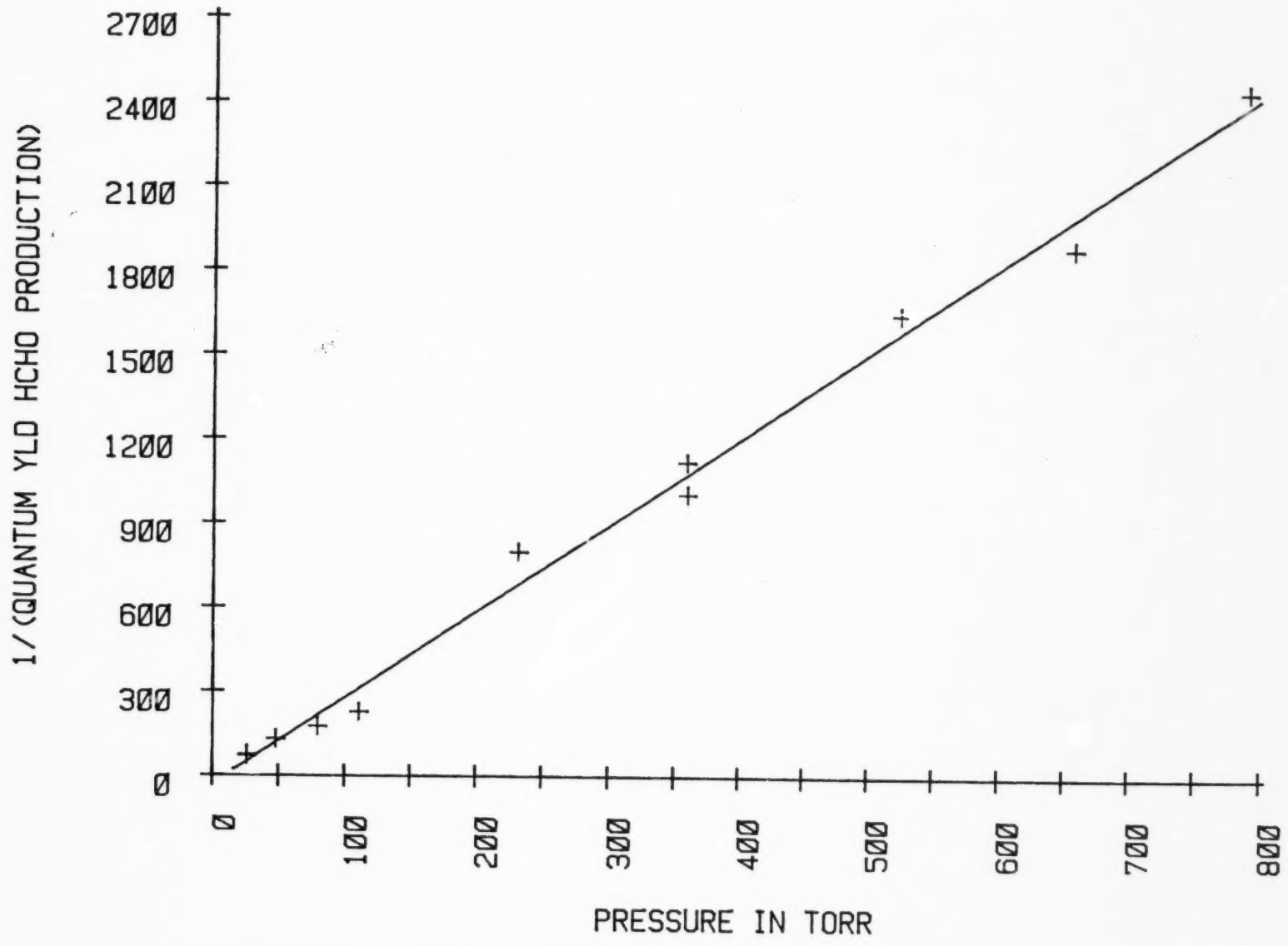
2700
2400
2100
1800
1500
1200
900
600
300
0
1/(QUANTUM YLD HCHO PRODUCTION)
0
100
200
300
400
500
600
700
800
PRESSURE IN TORR

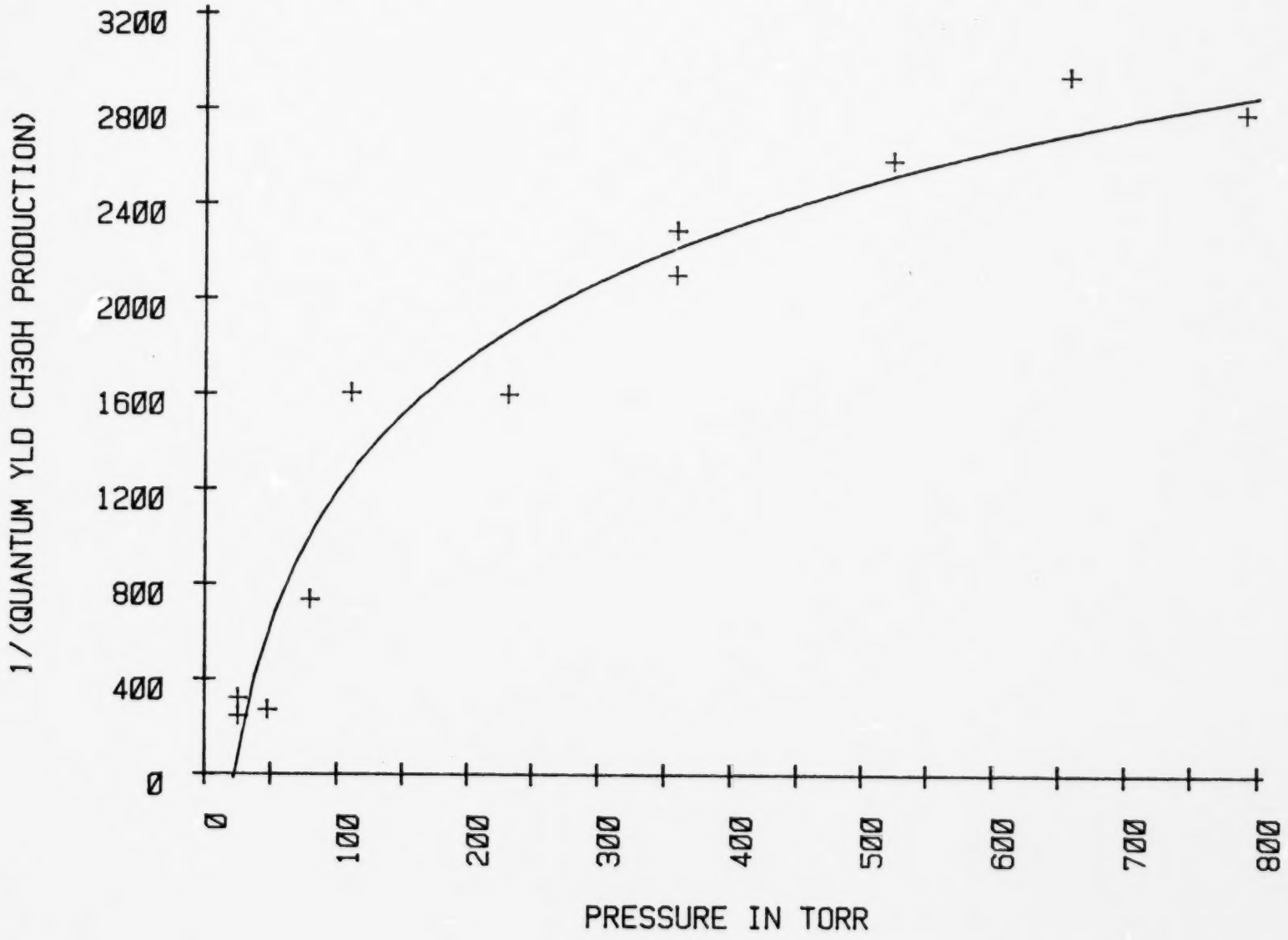
3200
2800
2400
2000
1600
1200
800
400
0
1/(QUANTUM YLD CH3OH PRODUCTION)
0
100
200
300
400
500
600
700
800
PRESSURE IN TORR